January 2014

Application Of Method Developed For The Identification And Quantification Of Polar Components In Organic Liquid Products Of Selected Crop Oils And Deciphering The Mechanistic Aspects Of Cracking

Ashwini Geetla

APPLICATION OF METHOD DEVELOPED FOR THE IDENTIFICATION AND QUANTIFICATION OF POLAR COMPONENTS IN ORGANIC LIQUID PRODUCTS OF SELECTED CROP OILS AND DECIPHERING THE MECHANISTIC ASPECTS OF CRACKING

by

Ashwini Geetla

A Thesis

Submitted to the Graduate Faculty

of the

University of North Dakota

in partial fulfillment of the requirements

for the degree of

Master of Science

Grand Forks, North Dakota

May

2014

This thesis, submitted by Ashwini Geetla in partial fulfillment of the requirements for the Degree of Master of Science from the University of North Dakota, has been read by the Faculty Advisory Committee under whom the work has been done and is hereby approved.

_____

Dr. Alena Kubatova (Chairperson)

_____

Dr. Evguenii Kozliak

_____

Dr. David T. Pierce

This thesis meets the standards for appearance, conforms to the style and format requirements of the Graduate School of the University of North Dakota, and is hereby approved.

_____

Wayne Swisher
Dean of the Graduate School

_____

Date

PERMISSION

Title Application of Method Developed for the Identification and Quantification of Polar Components in Organic Liquid Products of Selected Crop Oils and Deciphering the Mechanistic Aspects of Cracking

Department Chemistry

Degree Master of Science

In presenting this thesis in partial fulfillment of the requirement for a graduate degree from the University of North Dakota, I agree that the library of this University shall make it freely available for inspection. I further agree that permission for extensive copying for scholarly purposes may be granted by the professor who supervised my thesis work or, in her absence, by the chairperson of the department or the dean of the graduate school. It is understood that any copying or publication or other use of this thesis or part thereof for financial gain shall not be allowed without my written permission. It is also understood that due recognition shall be given to me and the University of North Dakota in any scholarly use which may be made of any material in my thesis.

Ashwini Geetla

4/28/2014

TABLE OF CONTENTS

LIST OF FIGURES

Figure Page

LIST OF TABLES

TABLE PAGE

ABBREVIATIONS

TGs	Triacylglycerides
OLP	Organic Liquid Product
BSTFA	*N, O-Bis(trimethylsilyl)trifluoroacetamide*
TMCS	Trimethylchlorosilane
TMAH	Tetramethyl Ammonium Hydroxide
DCM	Dichloromethane
GC-FID/MS	Gas Chromatography-Flame Ionization-Mass Spectrometry.
FAs	Fatty Acids
TIC	Total Ion Current
EIC	Extracted Ion Chromatogram
FID	Flame Ionization Detector

ACKNOWLEDGEMENTS

First I would like to express my sincere gratitude to my advisor Dr. Alena Kubatova for her innovative views, ideas, motivation, assistance and guidance throughout this research project. She has graciously given me her most valuable advice, time with patience and expertise throughout my research work and thesis writing. Without her guidance and help it would be impossible for me to complete this research work. I would also like to specially thank my co-advisor Dr. Evguenii Kozliak for his guidance, suggestions and many good advices and his patience during the correction of my thesis. I would also like to express my sincere gratitude to my thesis committee member Dr. David Pierce for his timely suggestions and valuable comments. I would like to thank Dr. Wayne Seames and Michael Linnen from Chemical Engineering Department for providing us with samples required for this study. I would like to thank my colleague Dr. Jana Stavova and Danese Stahl, Research Chemist in our lab, for training me on GC7890 and also for their valuable suggestions when needed.

Last but not least, I would like to express my deepest appreciation and love to my grandparents, parents, husband and friends for their constant support and encouragement along my life. You are the greatest power making me move forward throughout the years ever.

ABSTRACT

Pyrolysis is a fundamental thermochemical process that can be used to convert triacylglycerides (TGs) in crop oils into valuable chemicals that may replace petroleum products. Biofuels, complex mixtures containing hundreds of species, are generated by the pyrolysis of crop oils. Presence of fatty acids (FAs) will limit the applicability of plant oils as biofuels since they are corrosive and form wax-like crystals at a cloud point that would plug filters. However, short chain FAs have a high commercial value as byproducts of biofuel production. The understanding of mechanism of pyrolysis may reveal pathways for production of favorable products. These pathways are expected to depend on the type of TG feedstock with differing FA composition; for instance, the acyl chain length and number of double bonds.

Linear saturated FAs $<C_{11}$ were formed selectively, with a specific homological pattern featuring peaks at C_2-C_3, C_7 and C_9-C_{10}. The reaction pathways explaining formation are proposed. The relative abundance of these three groups of FAs varied among the feedstocks used due to variations in the double-bond pattern; i.e., the abundance of monounsaturated (oleic), diunsaturated (linoleic) and triunsaturated (linolenic) acids in the original TGs. Unsaturated FAs were recovered in small amounts only for the original TG-comprising FAs (C_{18}). The other group of minor products were C_5-C_{12} dicarboxylic acids. The observed product speciation and homology profiles were explained by the formation of acyloxyl biradicals as essential reactive intermediates.

CHAPTER 1

INTRODUCTION

1.1 Background

The rapid consumption of world's accessible petroleum reservoirs is due to rapid growth of population with increased industrialization and motorization.[1] Out of the total primary energy consumed in the world, fossil fuels account for 80%, of which 58% alone is used by the transportation sector.[2–4] Petroleum fuel reserves are diminished day by day and combustion of these fuels also cause environmental concerns resulting from emissions of CO_2, SO_2, and NO_X (where X is 1 or 2).[5–7] These problems stimulate the development and commercialization of alternative energy sources which are technically acceptable, economically competitive, environmentally friendly, and readily available.[5–7] Conversion of plant, algae or bacterial feedstocks, which primarily consist of TGs shown in Figure 1, represents a promising option for the production of fuels and chemicals.[8,9] Reaction products that are extracted from these feedstocks have similar fuel properties to that of petroleum based fuels except for their higher viscosity and low oxidative stability that must be verified before being converted into biofuel.[9] TGs are esters made up of three molecules of FA chains attached to a glycerol backbone.[10,11] The length of the FA chains and number of double bonds in TGs is varied depending on feedstock. The carbon chain typically contains an even number (12 to 24) of carbon atoms with up to three unsaturated bonds.[12] Even though relatively few crop oils were used in this study, similar properties are seen in other feedstocks.

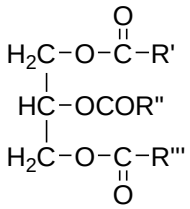

Figure 1. Basic structure of triaclyglyceride. R', R'' and R''' denote different FAs.[9]

1.2. Plant Oils

Plant oils consist mostly of TGs but also contain small amounts of free FAs. Table 1 shows FAs commonly occuring in plant oils. In addition, they contain some monoglycerides, diglycerides, and variable amounts of phospholipids, triterpene alcohols, carotenes, esterified sterols, chlorophylls, and other coloring matters and even trace amounts of metals.[11] Plant oils have high viscosity and lower volatilities, which cause formation of deposits in engines due to incomplete combustion and vaporization compared to conventional fuel.[13] The polymerization of unsaturated FAs at high temperatures, is an another issue resulting in agglomeration and gumming if the oils are used directly in engines.[14] Therefore, neat vegetable oils are not suitable for direct use as fuel. Instead they have to be modified under the right processing conditions in order to bring their combustion-related properties closer to those of petroleum fuel.[15] Pyrolysis is a fundamental thermochemical process that can be used to convert TGs into biofuels.[17]

Table 1. Common FAs found in plant oils. [16]

Trivial name	IUPAC name	$C_{n:b*}$
Saturated		
Capric acid	Decanoic acid	$C_{10:0}$
Lauric acid	Dodecanoic acid	$C_{12:0}$
Myristic acid	Tetradecanoic acid	$C_{14:0}$
Palmitic acid	Hexadecanoic acid	$C_{16:0}$
Stearic acid	Octadecanoic acid	$C_{18:0}$
Arachidic acid	Eicosanoic acid	$C_{20:0}$
Behenic acid	Docosanoic acid	$C_{22:0}$
Unsaturated		
Palmitoleic acid	9-Hexadecenoic acid	$C_{16:1}$
Oleic acid	9-Octadecenoic acid	$C_{18:1}$
Vaccenic acid	11-Octadecenoic acid	$C_{18:1}$
Gadoleic acid	9-Eicosenoic acid	$C_{20:1}$
Erucic acid	13-Docosenoic acid	$C_{22:1}$
Linoleic acid	9,12-Octadecadienoic acid	$C_{18:2}$
Linolenic acid	9,12,15-Octadecatrienoic acid	$C_{18:3}$
Arachidonic acid	5,8,11,14-Eicosatetraenoic acid	$C_{20:4}$

*'n' refers to the carbon length and 'b' the number of double bonds.

1.3. Pyrolysis

Pyrolysis is the process involving thermochemical cracking of organic macromolecules in the absence of oxygen. Thermal decomposition of TGs produces alkanes, alkenes, alkadienes, aromatics and carboxylic acids.[17] Pyrolysis is being used to convert biomass into OLP (bio-oil), solid (bio-char) and gas phase products.[17] The resulting bio-oil can be used as fuel or for the production of chemicals and other bio-based products potentially replacing petroleum products. Through the control of heating rates, reaction temperature, and residence times in the pyrolysis process, one can derive the various products can be derived that have a commercial value.[18] Figure 2 illustrates the products of pyrolysis and some potential product utilization.[19]

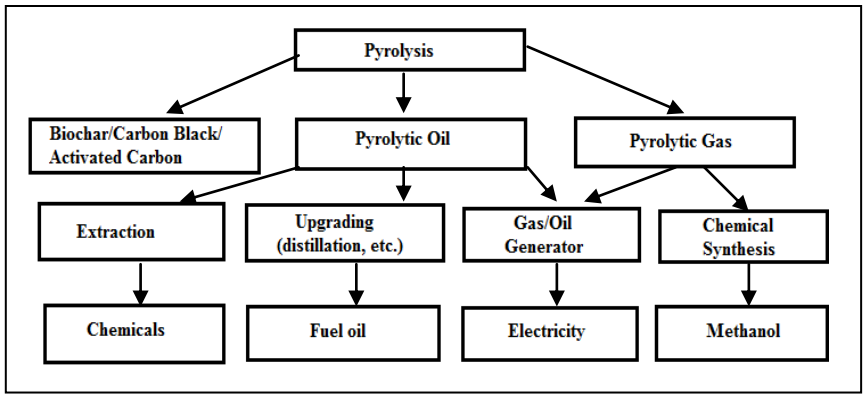

Figure 2. Potential product of pyrolysis of TG based feedstocks.[29]

Process parameters that have a major influence on the formation of products, are the pyrolysis temperature, heating rate, particle size, and residence time. Based on these parameters, pyrolysis is primarily divided into three types: conventional/slow pyrolysis, fast pyrolysis, and flash pyrolysis.[20] Types of pyrolysis and typical reactor configurations are presented in Table 2.[21]

Chemistry involved in pyrolysis is difficult to characterize because of the variety of reaction paths and the variety of reaction products. Pyrolysis can be performed either in the presence or absence of a catalyst.[17]

Table 2. Types of pyrolysis and typical reactor configurations.[21]

	Conventional	Fast	Flash
Operating conditions			
Heating rate (°C/s)	0.1-10	10-200	>1000
Particle size (mm)	5.0-50	<1	<0.2
Vapor residence time (s)	450-550	0.5-10	<0.5
Product yields (wt%)			
Liquid	~30	60-75	~80
Char	~35	15-25	~15
Gas	~35	15	~5
Reactor Configuration	Fixed bed	Ablation	Fluidized bed
	Vacuum	Auger	Circulating fluidized bed
		Fluidized bed	Downer
		Circulating fluidized bed	

1.4. Proposed Mechanisms of Thermal Degradation of TGs

Thermal decomposition of TGs is very complex due to formation of multiple products.[22- 23] The complexity increases as the feedstocks from plants consist of several TGs, which may react differently to form different compounds. A number of studies were conducted investigating the decomposition of saturated and unsaturated TGs with and without catalyst.[22-34]

In catalytic pyrolysis, the TGs primarily decompose into various organic compounds such as long chain FAs, ketones, aldehydes, and esters.[24] These first stage intermediates, long chain FAs fragments, are primarily formed either as acyloxyl radicals or acylium radicals through the decomposition of TGs.[25,26] The pyrolysis may occur in any of the three FA esters.[25-27] The acyloxyl and acylium radicals further undergo deoxygenation (decarboxylation and deketenization, respectively) yielding long-chain alkenyl radicals, shown in Figure 3.[28-29] These intermediate OLPs further break into a mixture of hydrocarbons, CO, CO_2 and water via various reactions, such as hydrogen transfer, β-scission, isomerization, aromatization, and cyclization reactions, not shown.[30,32] When using plant TGs with unsaturated FAs, cleavage occurs at allylic position to the double bond as shown in Figure 4.[24]

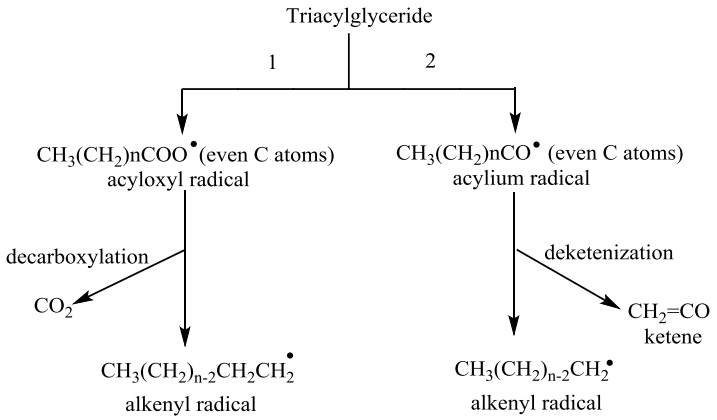

Figure 3. Thermal decomposition TGs.

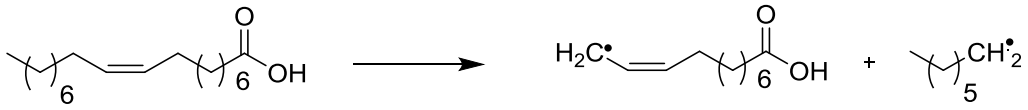

Figure 4. Allylic C-C bond scission.

Previously short-chain FAs were recovered in high yield in the OLP obtained upon non-catalyzed TG pyrolysis.[31] By contrast, the non-catalyzed TG pyrolysis was previously believed to yield long-chain FAs as the main products. Surprisingly, this process was shown to occur at 420–440 °C; temperatures that are lower than those required for the C-C bond scission.[31] However, a mechanism using the FA homology profiles was not reported to our knowledge.

1.5. Chemical Characterization of OLP

For effective evaluation of the OLPs for generation of fuels or chemicals it is essential to provide detailed characterization of OLP. The OLP contains a variety of compounds, such as traces of starting material (TGs), intermediate products (mono and di-carboxylic acids), hydrocarbons (aliphatic and aromatic), alcohols, ketones and some unidentified components.[31-34] Some of the OLP species are volatile and thus can be analyzed using GC-MS or GC-FID. However identification and quantification using GC-FID have certain limitations.[26] In identifying the species, the retention time of the standard may coincide with that of several species in the sample.[24] GC-FID or GC-MS has been previously employed for quantification using the normalization technique; however, a limitation of this approach is that the total area of the chromatogram may not represent 100% of the analyte due to non-eluted species.[35] Therefore, new analytical methods were needed to overcome these problems and obtain a complete characterization of TG pyrolysates.[34] A new suite of methods using GC-FID/MS was previously

developed enabling detailed identification and quantification of hundreds of species in TG pyrolysates.[31,33,36] One of the essential findings in previous studies was high abundance of short chain FAs (C_2-C_{11}).[32] While some other groups reported monocarboxylic acids previously, the reported acids were only long chain acids.[22,23] This omission was due to limited use of derivatization techniques and complexity of sample preventing identification.[31]

2. OBJECTIVES

The mechanistic aspects of pyrolysis significantly depend on the type of feedstock used since the physical and chemical properties of triglycerides are strongly dependent on FA composition. The presence of FAs in biofuels is detrimental because they are corrosive and form wax like crystals at cloud point and plug filters and fuel lines as temperature goes below the cloud point. Their presence will limit the applicability of plant oils as biofuels. However, these short chain FAs have high commercial value as byproducts, and their value decreases as the carbon chain length increases. This necessitates a comprehensive study of FAs in cracked plant oil samples.

In this work, we employed a method for the identification and quantification of FAs to compare and evaluate homology profiles in pyrolyzed organic liquid products of selected TG oils of varying composition. The goal of the study was to provide an understanding and mechanistic insights on formation of short FAs. OLP samples were generated and studied using two different pyrolysis systems. A large scale flow-reactor generated samples from TG mixtures comprising selected crops; that is, a system applicable to industrial setting. The interpretation of mechanism of pyrolysis was further confirmed using a system with online pyrolysis with GC-FID/MS.

3. EXPERIMENTAL SECTION

3.1. Chemicals

Dichloromethane (GC grade) was purchased from Fisher Scientific (Waltham, MA, USA). Bis(trimethylsilyl)trifluoroacetamide with trimethylchlorosilane (BSTFA +TMCS, 99:1) derivatization agent was purchased from Sigma Aldrich (St. Louis, MO, USA). 2-chlorotoluene was used as an internal standard (Sigma-Aldrich, St. Louis, MO, USA). For identification and quantification of OLPs, calibration mixtures consisting of carboxylic acids (0.1 to 680 µg/mL) and ketones (0.2 to 160 µg/mL) were prepared from the analytical grade standards shown in Table 4. Calibration data and plots for all the standards used are shown in Appendix C and D respectively. For online pyrolysis-GC/MS study, triolein was purchased from Sigma Aldrich (St. Louis, MO, USA). Tetramethyl ammonium hydroxide (TMAH) solution in methanol (25% w/w) was used as a derivatization agent for triolein. FAs C_5-C_{18}, shown in Table 6, were used as standards for the identification of pyrolyzed species of triolein.

3.2. Sample preparation

In this study we considered nine different feedstocks. Table 3 shows the complete composition of all feedstocks used in this study. Most of these feedstocks are triglyceride based except Jojoba oil which is a non-triglyceride based wax.[37] Jojoba oil consists of a mixture of esters of long chain linear alcohols and FAs, shown in Figure 5. The alcohol chain length may vary from C_{16} to C_{24}. $C_{18:1}$, $C_{20:1}$ and $C_{22:0}$ being the dominant species in FAs.

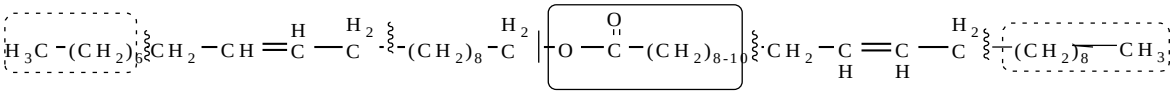

Figure 5. Jojoba chemical structure

The OLP samples were obtained from the UND Department of Chemical Engineering. All of these samples were pyrolyzed in a 20′ long x 0.18″ ID continuous tubular cracking reactor (TCR), constructed from a seamless, coiled stainless steel tube. For experimental data collection, the reactor was brought from ambient conditions to the desired operating temperature (435 °C), pressure (400 psi), and flow rate (3.5 mL/min). The reactor was allowed to reach steady state by flowing at least 300 mL of experimental oil through the reactor and maintaining a stable temperature, pressure, and flow rate during that time. At steady state, sample collection began and the reactor was allowed to operate for 45 minutes while a sample was collected. After 15 minutes of sample collection, the on-line GC procedure was initiated to determine the composition of the gas phase products for that sample. Each feedstock was collected as three separate fractions, and samples were saved for subsequent analysis.

Table 3. Original FA composition of all nine feedstocks.

Oil Feedstock (wt %) ($C_{x:y}$)**	10:0	12:0	14:0	16:0	18:0	18:1	18:2	18:3	20:0	20:1	22:0	22:1
Linseed[38]				6	2.5	19	24.1	47.4				
Camelina[39]				7.8	2.96	16.77	23.08	31.2	1.2	15.5		2.8
Canola[40]				4	2	60	20	10		2		2
Soybean[41]				11	4	24	54	7		~		~
Corn[42]				11.5	2.2	26.6	58.7	0.8	0.2			
Cotton[43]			0.8	24.4	2.2	17.2	55	0.3				
Cuphea[44]	81.9	3.2	4.3	3.7	0.3	3.6	2	0.3				
HOCO* (75%)[45]				4	2	75	22	10				
Jojoba[46]						10				66	14	

** Cx:y, x is the number of carbon atoms and y is the number of double bounds *HOCO – High oleic canola oil (75%). Soybean, corn and cotton oils are rich in linoleic acid. Canola and HOCO oil are rich in oleic acid. Camelina and linseed oils are rich in oleic, linoleic and linolenic acids. Cuphea oil is rich in decanoic acid.

For the GC analysis, the OLP samples (10 μL) and standards were derivatized with BSTFA+TMCS, 99:1 (200 μL) at 60 °C for 1 h. For the analysis of the OLP of cuphea, both the acid and ketone standards were derivatized with BSTFA+TMCS, 99:1 (200 μL) under the same conditions. After cooling to room temperature, DCM and 2-chlorotoluene (5 mg/mL) were added to make it to the final volume of 1 mL. The cuphea oil OLP samples were diluted 20-fold as the concentrations of produced FA10 was above the concentration of the highest calibration standard.

For the online pyrolysis with GC-MS (Py-GC/MS), the triolein standard was prepared in different concentrations ranging from 300 to 1000 ppm (w/v) in methanol, which were derivatized with TMAH (1 μL). Samples were introduced into a the pyrolysis quartz tube in small aliquot (1 μL) and analyzed using Py-GC/MS system. The experiments with triolein standard were performed with and without the derivatization agent. These experiments were conducted to get a preliminary idea about qualitative

characterization and to confirm our hypotheses obtained upon performing large scale experiments.

3.3. Instrumentation

The FA analysis of OLP samples was carried out as described previously using a GC-FID/MS (Agilent7890A GC, 5975C MS, Santa Clara, CA, USA) and equipped with an autosampler (7683 series).[34] The analyses were performed in a splitless mode (1 min), with the injection volume set to 0.2 µL. The GC separation was performed using a HP-5MS capillary column (60 m×250 µm×0.25 µm). Helium was used as a carrier gas at a constant flow rate of 1.1 mL/min. The GC oven temperature started at 35 °C with hold for 5 min, followed by 20 °C/min gradient to 300 °C and final hold for 12 min. The MS was used for quantification with the transfer line kept at 300 °C. The MS data (total ion chromatogram, TIC) were acquired in the full scan mode (*m*/*z* of 33–550) using the electron ionization (EI) of 70 eV. The accurate determination of solvent delays was based on simultaneously acquired GC-FID data; this prevented detection of solvent and derivatization reagents by MS. The performance of the system was regularly checked using a custom-made test mix. Data collection and processing were performed using GC Chemstation software. To verify the content of higher molecular weight species, such as unpyrolyzed TGs, diglycerides, and monoglycerides, the analyses were also performed on a high temperature (HT) column using the instrumental setup specified above with a programmable temperature vaporizer (PTV) injector. The PTV program was operated in the splitless mode (2.6 min), started at 40 °C, hold for 0.7 min, followed by 720 °C/min gradient to 380 °C and final hold for 10 min. Injector volume was set to 0.2 µL. The HT analysis was performed on a DB-1HT capillary column (15 m×250 µm×0.1 µm). The GC

oven temperature started at 35 °C with hold for 2.6 min, followed by 15 °C/min gradient to 230 °C, and again ramped at 20 °C/min to 380 ° C, and final hold for 10 min. The MS-TIC data were acquired in the full scan mode (*m*/*z* of 70–750) using the EI of 70 eV.

The online Py-GC/MS experiments with triolein were performed using a pyroprobe model 5200 (CDS Analytical, Inc., Oxford, PA, USA) connected to the split/splitless injection port of Agilent 7890GC with a 5975C MS through a heated transfer line. The pyroprobe was operated at ambient pressure. All experiments were carried out in an inert atmosphere using ultra-high purity helium as a carrier gas. The quartz tubes for samples were filled with quartz wool which was positioned at the center of the quartz tube. The quartz tube was pre-cleaned by placing it in the Pt wire coil filament at 1200 °C for 10s. After cooling, a droplet of triolein (either neat or diluted) was introduced onto the quartz wool using a syringe or the plunger tip. All the samples were dried at 80 °C for 120 s before introducing them into the pyroprobe. Upon the run initiation, the pyroprobe interface was heated from the standby temperature (40 °C) to 300 °C at a maximum heating rate. The interface was heated in order to avoid the condensation of analytes coming from the pyrolysis tube. The pyrolysis temperature was altered from 750 °C to 450 °C (30 s) to understand the pyrolysis behavior at different temperatures. Initial experiments were performed at higher pyrolysis temperature in order to avoid potential clogging of the transfer line with incompletely pyrolyzed species. The analytes evolving from the pyrolysis tube were trapped onto the Tenax desorption trap with the standby temperature of 40 °C. The desorption trap was then rapidly heated to 300 °C and left there for 180 s. Trapping the analytes before introducing into GC enabled focusing the chromatographic peaks and hence improve the separation efficiency. The

pyroprobe isothermal zones (i.e., valve oven and GC transferline) were maintained at 350 °C. The GC injector was operated in a split mode (10:1) at 300 °C. The GC separation was performed using a HP-5MS capillary column (60 m×250 µm×0.25 µm). Helium was used as a carrier gas at a constant flow rate of 1.1 mL/min. The GC oven program started at 80 °C with hold for 5 min, followed by 20 °C/min gradient to 350 °C and final hold for 5 min. The temperature of the MS transfer line was kept at 300 °C.

3.4. Data Processing

The quantification and identification of OLP samples were performed using GC-MS Chemstation, the *m*/*z* target ions of trimethylsilated mono- and dicarboxylic acids were reported previously and are listed in Table 4.[33] Apart from mono- and dicarboxylic acids; ketones and unsaturated carboxylic acids were also detected. Their retention times, target ions and confirmation ions which are used for quantification and identification of respective species are also listed in Table 4. Compounds for which standards were not available were quantified using calibration parameters of the nearest standard representing the corresponding class of compounds. Table 5 shows the names of standards used for quantification, retention time, target ions and confirmation ions for those standards that were not available. Results are reported as an average with one standard deviation (n=3). The analytes of pyrolyzed triolein were identified using the methylate standards of monocarboxylic acids (Table 6) based on the retention time, and the matching MS spectra with NIST 05 spectral library.

Table 4. List of mono, di-carboxylic acids and ketones studied with their, suppliers' name, target ions, and confirmation ions are provided for trimethylsilylated compounds used in GC-MS analysis.

Analyte	Manufacturer*	Target ion (m/z)	Confirmation ions (m/z)	
Formic acid	Fluka	103	75	45
Acetic acid	Sigma-Aldrich	117	75	73
Propanoic acid	Acros	131	75	73
Butanoic acid	Acros	145	117	75
Valeric acid	Acros	159	129	117
Hexanoic acid	Acros	173	129	117
Heptanoic acid	Acros	187	129	117
Octanoic acid	Acros	201	129	117
Nonanoic acid	MP.Biomedicals	215	129	117
Decanoic acid	Acros	229	129	117
Undecanoic acid	Acros	243	129	117
Dodecanoic acid	Alfa Aesar	257	129	117
Tridecanoic acid	MP.Biomedicals	271	129	117
Tetradecanoic acid	Fluka	285	129	117
Pentadecanoic acid	Acros	299	129	117
Hexadecanoic acid	Acros	313	129	117
Heptadecanoic acid	Alfa Aesar	327	129	117
Octadecanoic acid	Acros	341	129	117
Nonadecanoic acid	Sigma-Aldrich	355	129	117
Eicosanoic acid	Acros	369	129	117
Heneicosanoic acid	Fluka	383	129	117
Behenic acid	Sigma-Aldrich	397	129	117
Tricosanoic acid	Sigma-Aldrich	411	129	117
Tetracosanoic acid	Acros	425	129	117
2-Octenoic acid	Pfaltz and Bauer	199	129	117
Oleic acid	Sigma-Aldrich	339	129	117
Suberic acid	Acros	303	147	117
Sebacic acid	Sigma-Aldrich	331	147	117
2-Undecanone	TCI America	58	127	112
9-Heptadecanone	TCI America	238	155	127
10-Nonadecanone	TCI America	266	155	127
11-Heneicosanone	TCI America	294	155	127

* Location of the chemicals purchased from, Fluka (St. Louis, MO, USA), Sigma-Aldrich (St. Louis, MO, USA), Acros (Fair Lawn, NJ, USA), Pfaltz and Bauer (Waterbury, CT, USA), Alfa Aesar (Ward Hill, MA, USA), MP. Biomedicals (Santa Ana, CA, USA), TCI America (Portland, OR, USA).

Table 5. List of unsaturated mono, di-carboxylic acids and ketones, for which standards were not available, with analyte quantified as, retention time (tr) and target and confirmation ions.

Analyte	Quantified as	tr (min)	Target ion (*m/z*)	Confirmation ions (*m/z*)	
Hexenoic acid	2-Octenoic acid	13.45	171	129	117
Heptenoic acid	2-Octenoic acid	14.1	185	129	117
Nonenoic acid	2-Octenoic acid	15.61	213	129	117
Decenoic acid	2-Octenoic acid	16.23	227	129	117
Undecenoic acid	2-Octenoic acid	16.82	241	129	117
Dodecenoic acid	2-Octenoic acid	17.38-17.44*	255	129	117
Tridecenoic acid	2-Octenoic acid	17.92-17.97*	269	129	117
Tetradecenoic acid	2-Octenoic acid	18.44-18.79*	283	129	117
Eicosenoic acid	Oleic acid	21.49-21.73*	367	129	117
Erucic acid	Oleic acid	22.93-23.19*	395	129	117
Pentanedioic acid	Suberic acid	15.39	261	147	117
Heptanedioic acid	Suberic acid	16.63	289	147	117
Nonanedioic acid	Suberic acid	18.2	317	147	117
Undecanedioic acid	Suberic acid	19.2	345	147	117
Dodecanedioic acid	Suberic acid	19.7	359	147	117
Dodecanone	2-Undecanone	15.35	72	112	127
Tridecanone	9-Heptadecanone	15.93	86	127	143
Tetradecanone	9-Heptadecanone	16.51	100	127	143
Pentadecanone	9-Heptadecanone	17.08	114	127	155
Hexadecanone	9-Heptadecanone	17.63	128	127	155
Octadecanone	9-Heptadecanone	18.66	156	127	155
Docosanone	11-Heneicosanone	20.91	170	127	155
Tricosanone	11-Heneicosanone	21.42	226	127	155
Pentacosanone	11-Heneicosanone	22.94	254	127	155

*Several isomers were seen within the specified time range

Table 6. List of methylsilylated monocarboxylic acids with their retention times, target ion and confirmation ions.

Analyte	tr (min)	Target ion (*m/z*)	Confirmation ions (*m/z*)		
Valeric acid	7.205	85	43	57	74
Hexanoic acid	8.537	99	43	57	74
Heptanoic acid	9.851	113	43	57	74
Octanoic acid	10.988	127	43	57	74
Nonanoic acid	11.934	141	43	57	74
Decanoic acid	12.742	157	115	129	143
Undecanoic acid	13.455	169	129	143	157
Dodecanoic acid	14.101	183	129	143	157
Tridecanoic acid	14.699	197	129	143	157
Tetradecanoic acid	15.262	211	129	143	157
Pentadecanoic acid	15.797	225	129	143	157
Hexadecanoic acid	16.304	239	129	143	157
Heptadecanoic acid	16.789	253	129	143	157
Octadecanoic acid	17.257	267	129	143	157

Manufacturer information for these standards is same as that of in Table 4.

4. RESULTS AND DISCUSSION

4.1. Characterization of OLPs

To understand the mechanistic aspects of TG cracking and formation of FAs, nine different feedstocks were studied, shown in Table 3. Some of the feedstocks used have similar and some have different chemical composition. For example, soybean, corn, and cotton oils are rich in linoleic acid ($C_{18:2}$) except that cotton oil have a slightly higher content of palmitic acid (Table 3). In contrast, canola oil is rich in oleic acid ($C_{18:1}$) and high oleic canola oil (HOCO) has a similar composition to that of canola except the oleic acid content (75 vs 60 wt %). Cuphea is different from other feedstocks featuring a large content of decanoic acid. Jojoba oil is the only feedstock, which is a wax while all others are triglyceride based. Chromatograms and summary of data in mol % of all OLP samples are presented in Appendix A and B respectively.

4.1.1. Evaluation of Method Repeatability

First, we studied the repeatability of pyrolysate preparation performed at the UND Chemical Engineering Department. Soybean oil OLP replicates were generated on the same day (i.e., collected sequentially), at the beginning and at the end of several pyrolysis experiments, and also on different days. In addition, one of the samples was prepared (derivatized) in triplicate for GC analysis to check for derivatization repeatability, and one of the samples was injected three times at different positions in a sequence and also on different days to check the repeatability of GC procedure. Figure 6 (a, b and c), shows the repeatability of pyrolysates, GC and derivatization respectively.

In all three cases, the replicates were found to be repeatable with the relative standard deviation less than 10%.

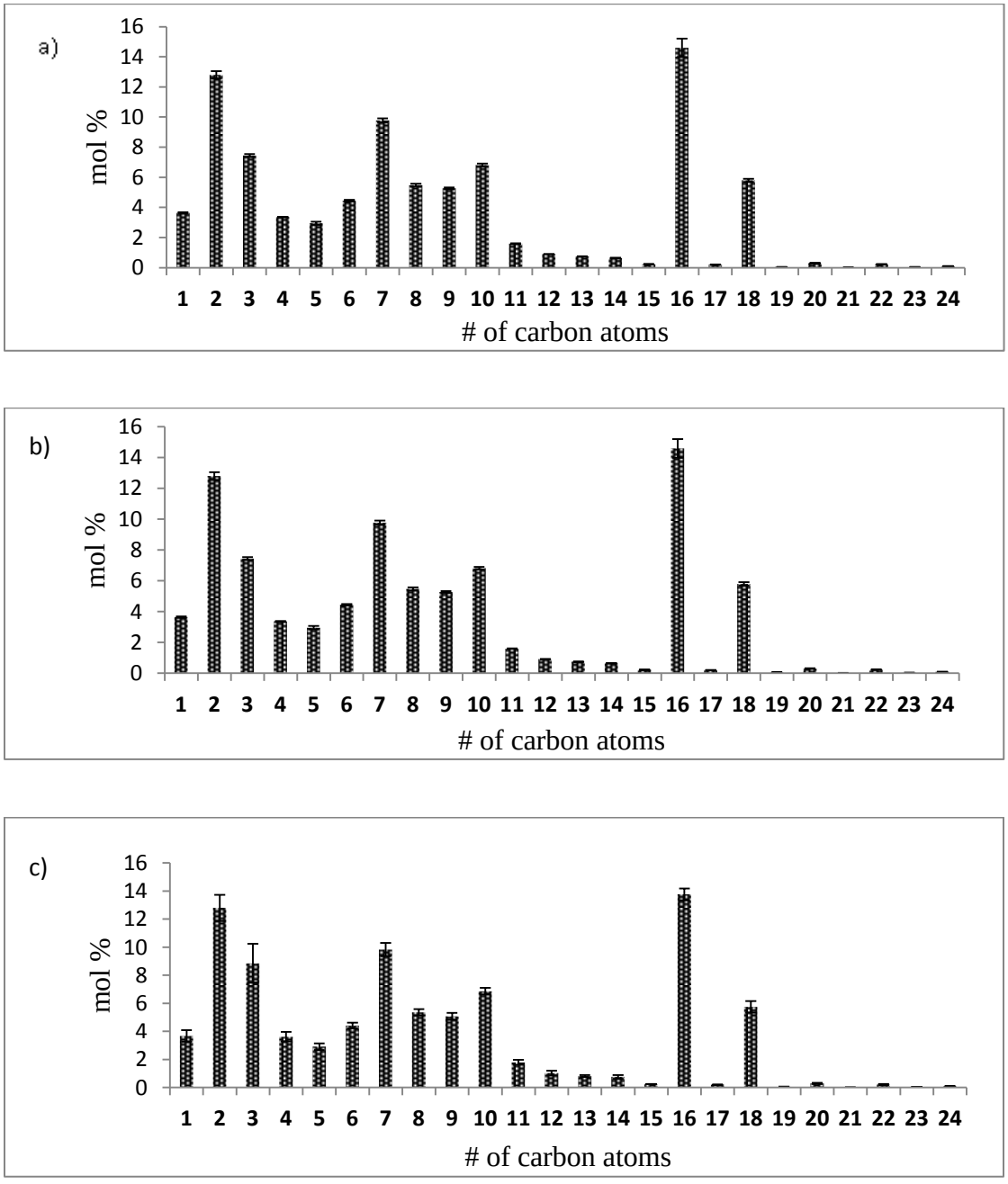

Figure 6. Evaluation of repeatability a) GC analysis b) derivatization and c) pyrolysis experiments of OLPs of soybean oil. The data are presented as mean value with standard deviation representing uncertainty.

4.1.2. FA Homology Profiles of Various Feedstocks with Similar Chemical Composition

Thermal decomposition of all the feedstocks studied resulted in the formation of monocarboxylic saturated FAs. In addition, monounsaturated and dicarboxylic acids were observed in all the feedstocks. Only in the OLP of cuphea oil ketones were observed.

4.1.2.1. Monocarboxylic Saturated FAs

The FA homology profiles for the feedstocks of similar composition (soybean, corn and cotton oils) rich in linoleic acid and those of different composition (soybean, canola and linseed oils) rich in linoleic, oleic and linolenic acids respectively, are shown in Figure 7. The three FA homology profiles in Figure 7a and b show similar trend (with peaks for C_2, C_7, C_{10} and C_{16}), as they all have a similar double bond pattern. However, the abundance of FAs differs. Apparently this is due to the change in the abundance of original FA composition within TGs. Longer chain acids such as C_{16} and C_{18} are noticeable in all charts indicating the presence of remnants of the original saturated FAs of TGs.

In Figure 7a, the trend is similar for all the three feedstocks except cotton oil, which has a relatively high amount of C_{16}. As mentioned above, this is expected because of the high amount of C_{16} FA in the original cotton oil feedstock. In Figure 7b, all of the three feedstocks exhibit similar trends except canola oil having a high amount of C_{10}, which might be due to the presence of high amount of $C_{18:1}$. This is also supported by an even higher amount of C_{10} for HOCO (75 %) which has an increased abundance of original $C_{18:1}$ compared to canola oil (shown in Figure 8c). Besides these apparent trends, we have observed a selectivity in pyrolysis in both the charts, shown in Figures 7 a, b by

a greater abundance of C_2-C_3, C_7 and C_9-C_{10} peaks. This confirms that the pyrolysis is not random but has some selectivity based on the original composition of the feedstocks used. The formation of these specific FAs may be explained based on the three paths shown below in Figures 8-12.

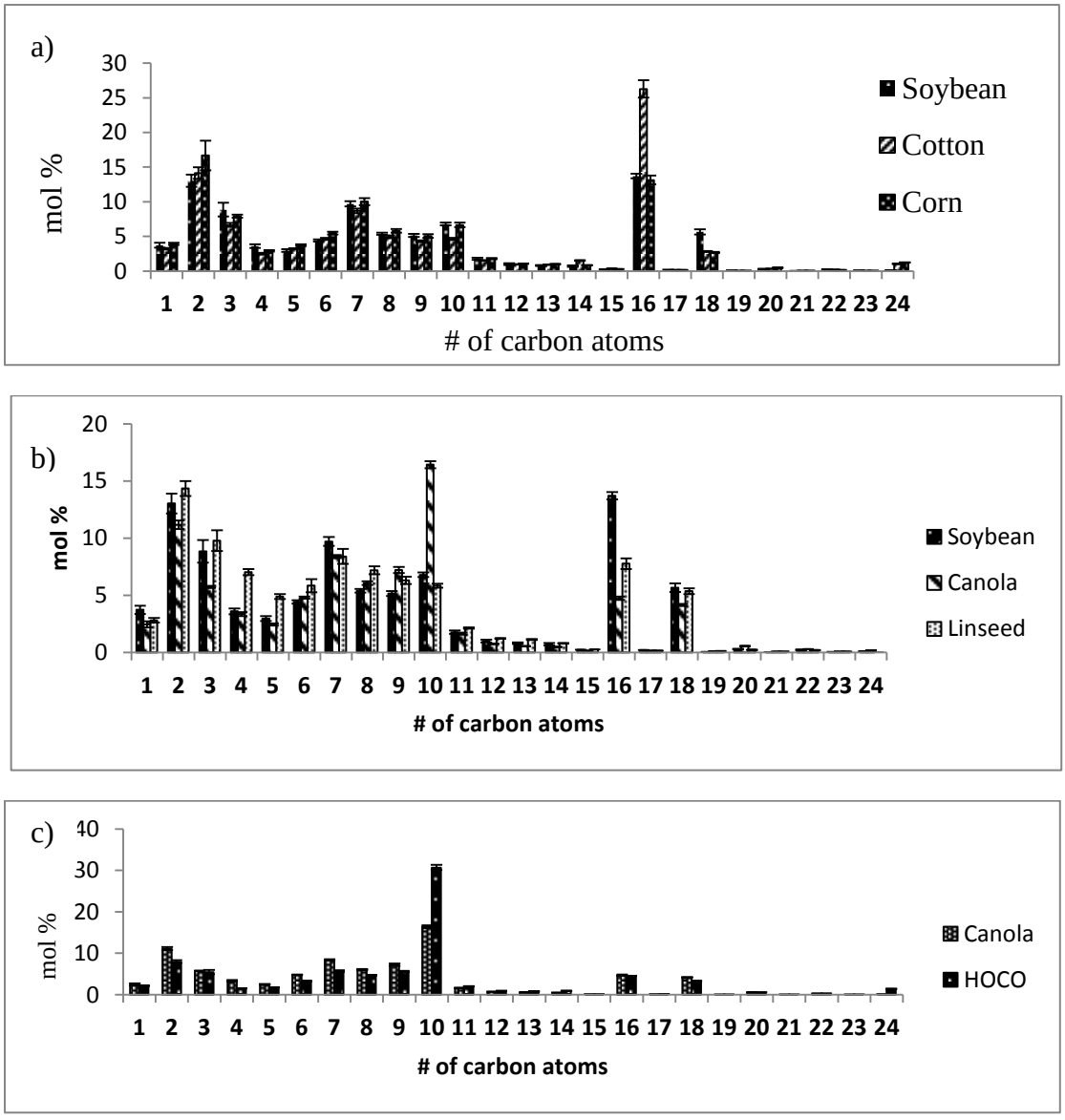

Figure 7. Saturated FA homology profiles of OLPs from feedstocks with similar chemical composition: a) rich in linoleic acid b) rich in linoleic, oleic, and linolenic acids respectively and c) HOCO has more oleic acid than canola oil.

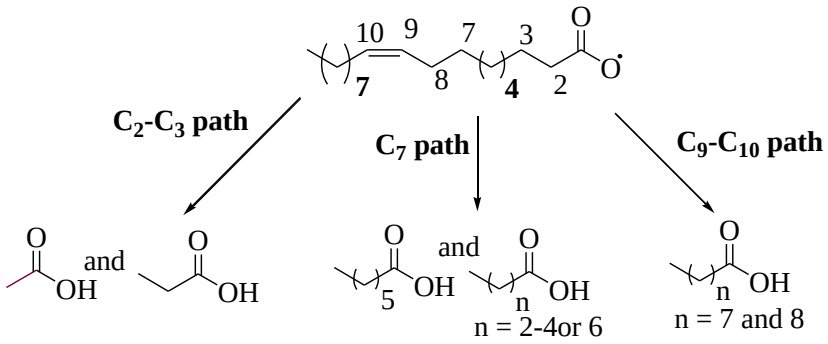

Figure 8. Three paths of acyloxyl radical pyrolysis

In the C_7 path, the cleavage of C-C bond in acyloxyl radical would occur at the allylic position to the double bond result's in the formation of C_7 saturated FA and/or C_{11} unsaturated FA. However, no monounsaturated (C_{11}) FAs were observed whereas the complementary C_7 hydrocarbons were detected in significant amounts. A plausible explanation for the formation of these pyrolysis products could be that the C-C bond scission on the ω-side of the double bond facilitates the further pyrolysis of the remaining FA fragment to remove the fragment which contains the double bond as shown in Figure 9.

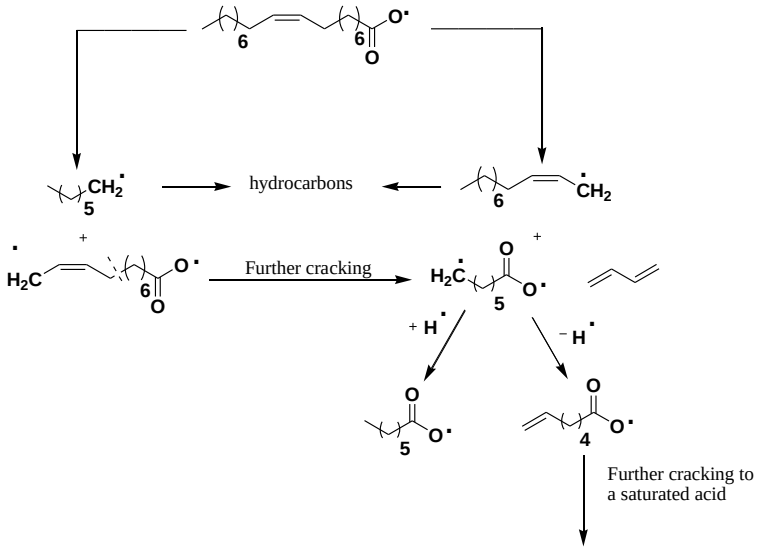

Figure 9. Proposed C_7 fragmentation pathway.

The C_9-C_{10} path was observed in canola oil with a higher abundance of oleic acid than linoleic acid, even though the amount of linoleic acid was still significant. According to this path, the ω-9 double bond scission occurs between C_9 and C_{10} in either oleic or linoleic or linolenic acids. However, this pyrolysis pathway may not be possible as sp^2C=sp^2C and sp^3C-sp^2C bond energies are stronger than the characteristic sp^3C-sp^3C bong energy. A possible explanation for this path is shown in Figure 10. Prior to the cleavage of the ω-9 double bond (C_9=C_{10}), this bond undergoes hydrogenation with highly active hydrogens, which are formed in the pyrolysis process of TGs. Following the hydrogen addition to the double bond, most of the hydrogen molecule's transferred kinetic energy would be localized near the former double bond triggering the concomitant sigma bond cleavage (either between the same carbon atoms, C_9 and C_{10}, or those adjacent to them)as depicted in Figure 10. As kinetic energy of the system is directly proportional to temperature, this pyrolysis pathway is feasible at high temperatures. The formation of these highly active biradicals further facilitates the C-C pyrolysis reactions and finally leads to stable fragments via hydrogen transfer or cyclization reactions.

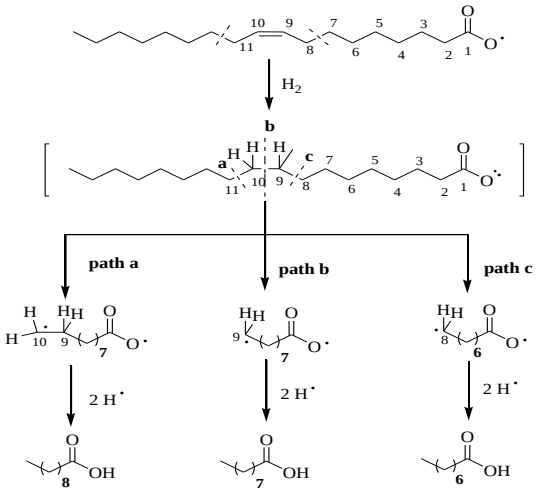

Figure 10. C_9-C_{10} fragmentation pathway (Oleic acid fragmentation).

Canola oil also contains significant amounts of linoleic acid although oleic acid is more abundant. In the case of linoleic acid the cleavage would most likely occur at ω-10 sigma bond as it is also allylic position to the ω-6 double bound. This could be also the reason why C_{10} FA is slightly excess over C_9 FA. For soybean the process appears to be more selective towards hydrogenation of ω-6 double bond leading to the formation of C_7 FA.

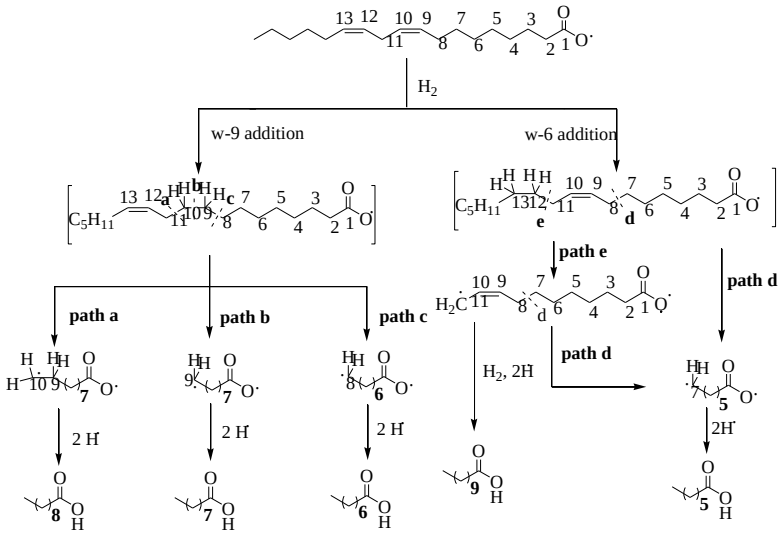

Figure 11. C_9-C_{10} fragmentation pathway (Linoleic acid fragmentation).

The occurrence of acetic and propionic acids was most pronounced in all the pyrolysis products. The formation of these two short chain acids can be explained by McLafferty rearrangement of acyloxyl free radicals (Figure 12).

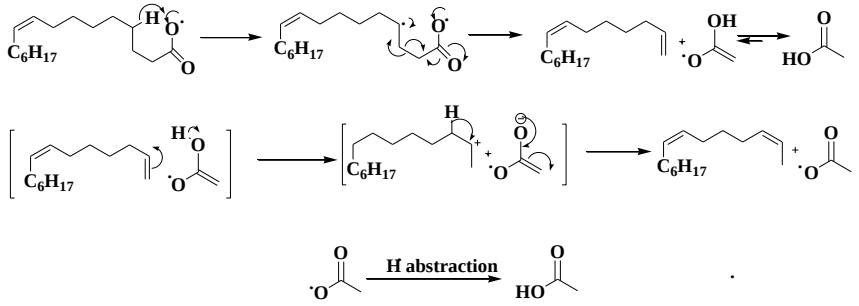

Figure 12. C_2-C_3 fragmentation pathway (McLafferty rearrangement of acyloxyl free radicals).

4.1.2.2. Mono unsaturated FAs

Figure 13 shows the unsaturated FA profile (totals of all unsaturated FAs for each Carbon No.) for the OLPs with similar composition (panel a) and with different composition (panel b). In both the charts, except for camelina oil, it can be seen that only $C_{18:x}$ is found to be formed in larger amounts and all the other unsaturated FAs are with very low abundance. This could be due to the presence of $C_{18:x,}$ could be either oleic ($C_{18:1}$), or linoleic ($C_{18:2}$) or linolenic acid ($C_{18:3}$), in all the original composition of the feedstocks. This means that some $C_{18:x}$ fragments were left unpyrolyzed. In Figure 13b, camelina oil has both $C_{18:x}$ and $C_{20:x}$ in abundance as it has them in its original composition. Several isomers of ecosenoic acid were observed in pyrolyzed camelina oil. Also several unsaturated acids were found in trace amounts, which show that these are unstable under pyrolysis conditions.

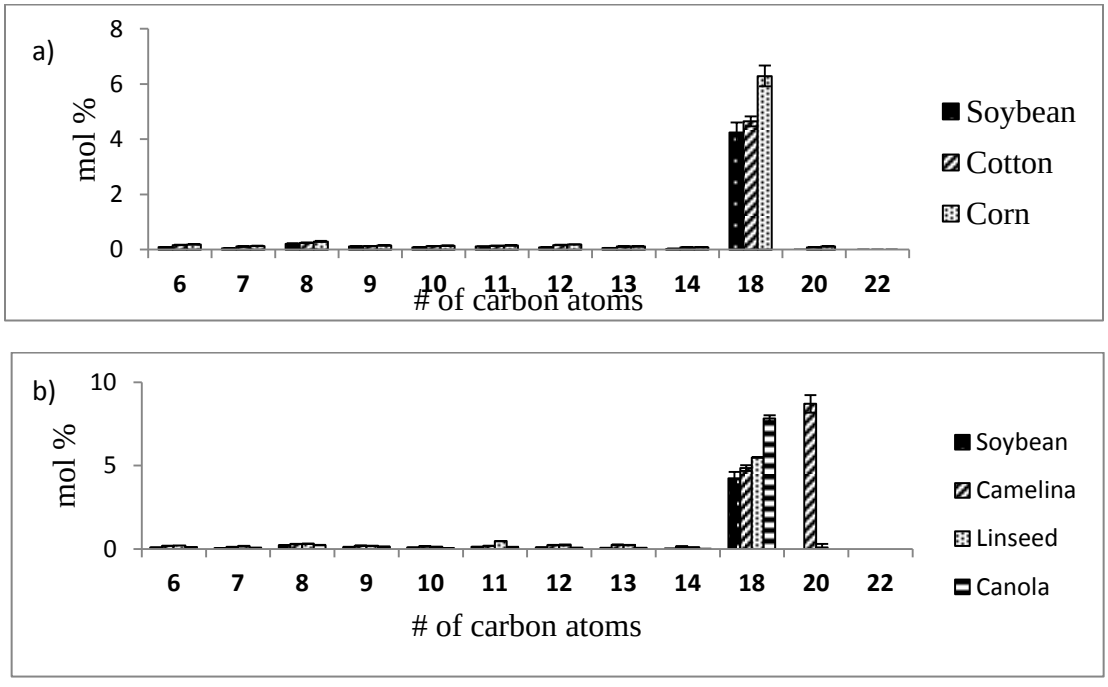

Figure 13. Unsaturated FA composition of feedstocks with . a) rich in linoleic acid b) soybean rich in linoleic, and camelina and linseed are rich in oleic, linoleic and linolenic acids and canola rich in oleic acid.. (totals of all unsaturated FAs for each Carbon No.)

4.1.2.3. Dicarboxylic acids

` Several dicarboxylic acids ranging from C_5 to C_{12} were observed in all the pyrolyzed feedstocks (representative profiles of dicarboxylic acids are shown in Figure 14). Dicarboxylic acids may be formed by a 'tail to tail' recombination of acyloxyl radicals forming a new C-C bond, C_{10} being the most abundant peak of all those. C_{10} could be formed by the 'tail to tail' recombination of C_4 and C_6 acyloxyl radicals. Also none of dicarboxylic acids with higher carbon numbers are seen, which suggests that the free radicals with lower abundance are prone to a 'tail to tail' collision. This means that free radical recombination is limited by entropy, larger size FA radicals with high abundance will have lower probability. There were no smaller, < C_4, dicarboxylic acids formed by paring the smaller FA radicals like C_2 and C_3. These two FAs are formed through McLafferty rearrangement which does not involve any unpaired electrons located at the terminal carbon atoms.

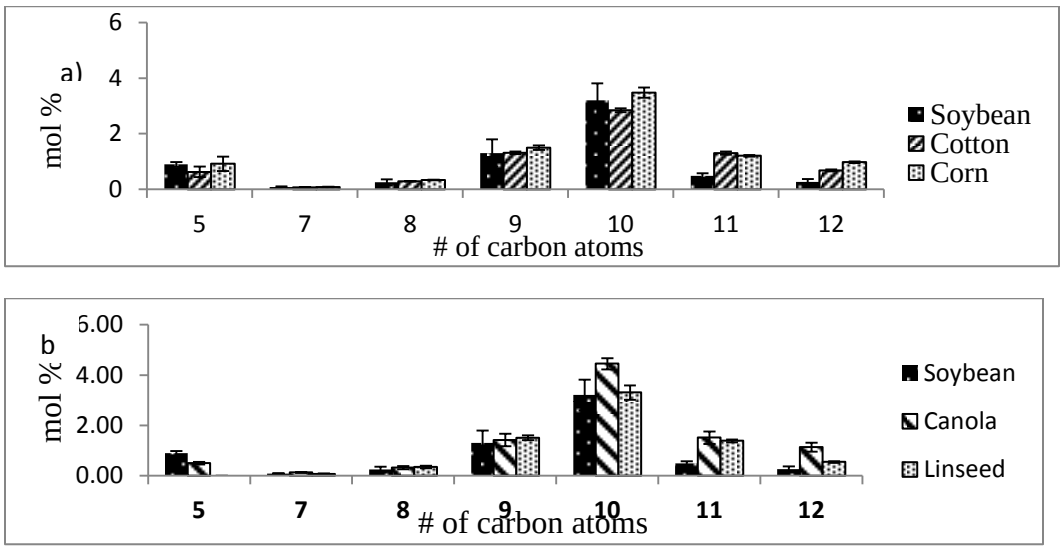

Figure 14. Dicarboxylic acids composition of feedstocks a) rich in linoleic acid b) soybean rich in linoleic, canola rich in oleic acid, and camelina rich in oleic, linoleic and linolenic acids (totals of all unsaturated FAs for each Carbon No.)

4.1.3. FA Homology Profiles of Feedstocks with Different Chemical Composition

4.1.3.1. Jojoba vs Other Feedstocks

Jojoba oil, being a non glycerol based feedstock, still yielded a similar homology profile to that of the glycerol based oils as, shown in Figure 15. Jojoba oil having a high content of $C_{18:1}$ in its original feedstock led to the formation of high amounts of C_{10} compared to C_7 acid. In addition, the formation of longer chain acids like C_{16} and C_{18} was significantly lower when compared to soybean and canola (Figure 15). This is because they are no original C_{16} and C_{18} saturated acids present in the original feedstock composition.

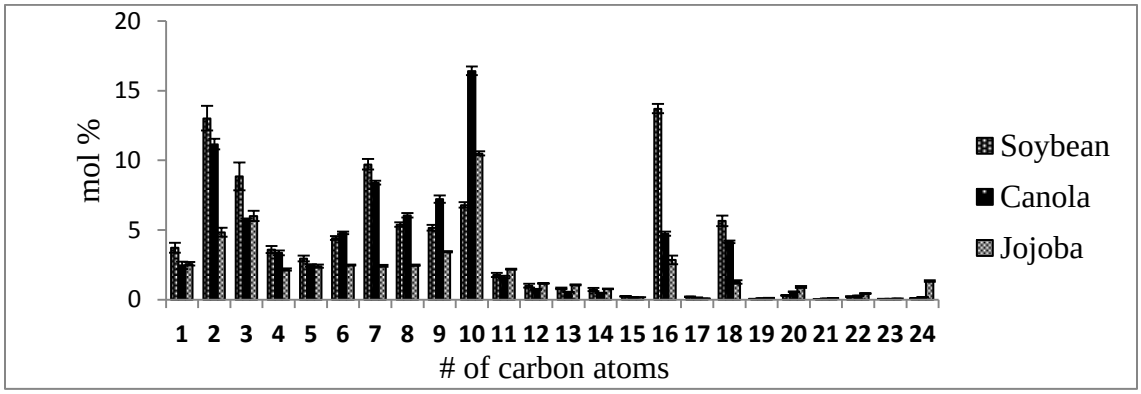

Figure 15. Comparison of saturated FAs of jojoba with soybean and canola OLPs.

4.1.3.2. Cuphea vs Other Feedstocks

Cuphea oil is unique in a way that it has 80% of C_{10} in its original feedstock and small amount of $C_{18:1}$, shown in Table 3. Figure 16 demonstrates the formation of C_{10} acid as the highest peak after cracking, in cuphea oil, which may originate both from the original saturated FA C_{10} in TG and from $C_{18:1}$. The other acids are found in very low concentrations. This suggested that only limited FA pyrolysis occurred when compared to soybean and canola oils.

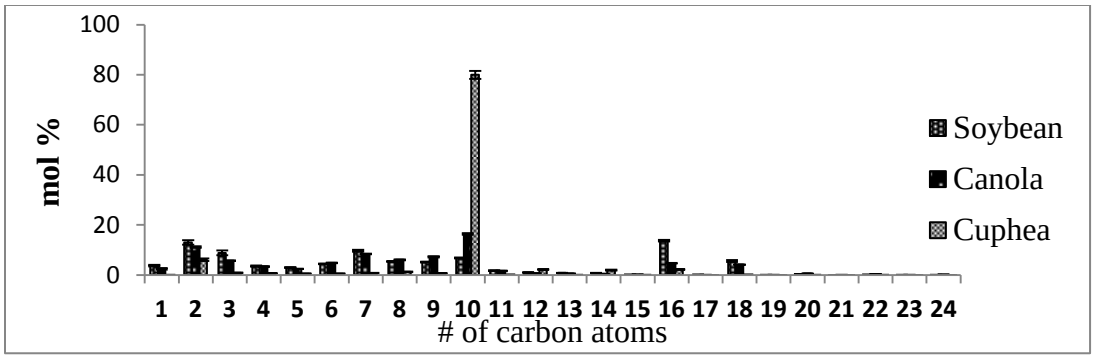

Figure 16. Comparison of saturated FAs profiles of cuphea, soybean and canola OLPs.

Beside the carboxylic acids we have successfully identified several previously unreported compounds, ketones. All these compounds had common ions of 155 and 127 *m/z* and eluted in a homological pattern (i.e., in regular interval with molecular ions of 14 amu apart), shown in Figure 17a. One of the most abundant peaks was identified with NIST 05 spectral library; the mass spectrum for this peak is shown in Figure 17b. The identity of ketones was then confirmed using available standards, which were also used for quantification. The % mole distribution of ketones found in cuphea oil is shown in Figure 17c. The expected mechanism of ketone formation may be through degradation of two carboxylic acids forming a ketone in the presence of a metal oxide catalyst by removing water and CO_2 molecules. However in our work no catalyst was added, still the metal oxides could be present in the stainless steel tube wall of the tubular cracking reactor. Thus a significant surface area of the reactor may be sufficient for metal sites to catalyze the reaction. Ketone C_{19} was the most prominent peak, which was expected as C_{10} FA was the major acid formed. Also none of the lower ketones were observed as it is much less likely that a vapor phase ketonization will occur. The vapor phase keeps the molecules far apart, and it makes them difficult to react in the presence of a metal oxide.

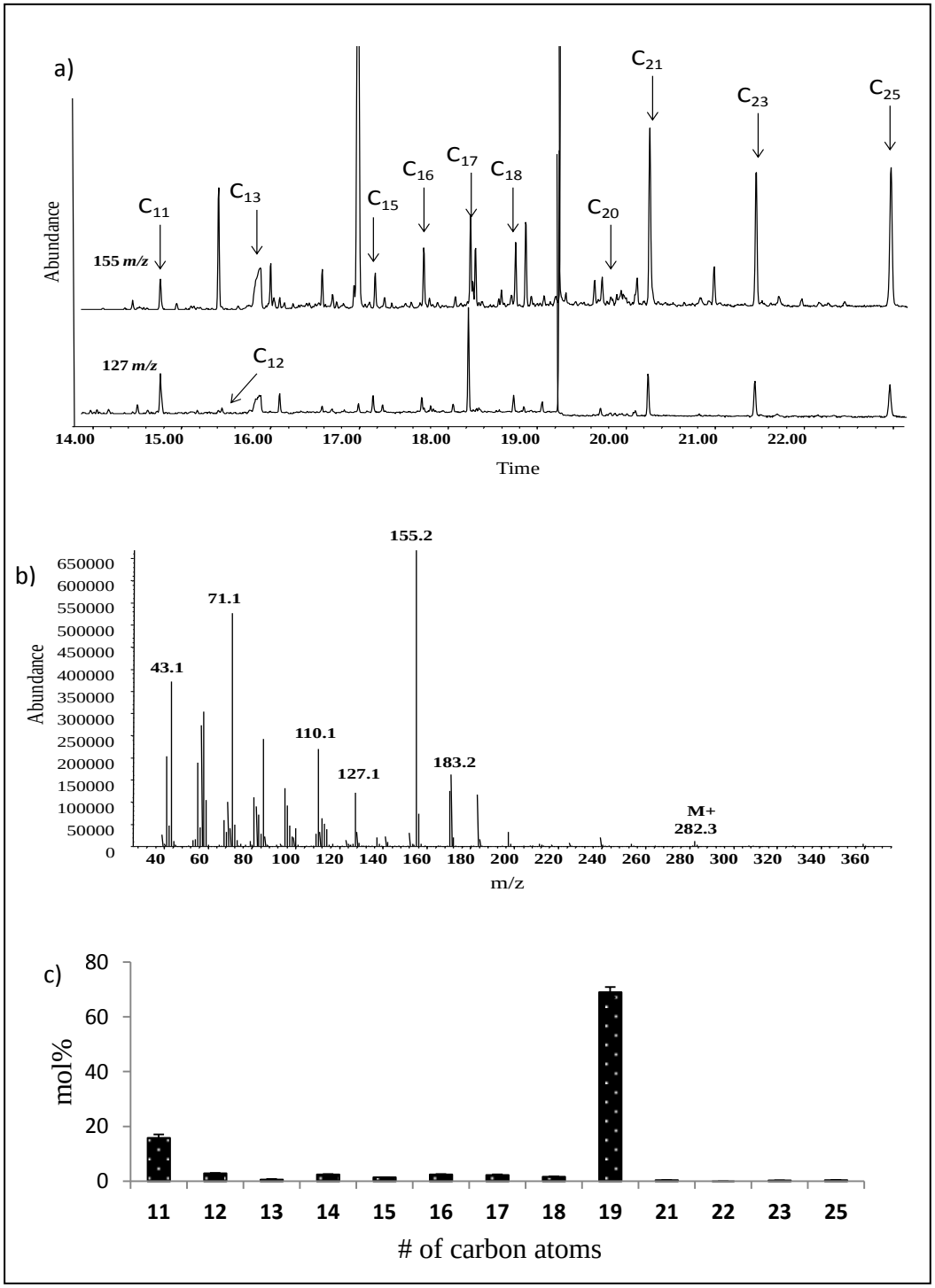

Figure 17. Occurrence of ketones in pyrolyzed cuphea sample: a) EIC of cuphea sample using ions (155, 127 *m/z*) b) mass spectrum of 10-nonadecanone c) mol% distribution.

4.2. Pyrolysis of Model Compound - Triolein

We have first optimized the method of sample introduction, as an excessive concentration may saturate the system and cause a carryover, while an insufficient concentration may be affected by active sites on the system resulting in a limited response as well as solvent may affect the reaction.

Thus first we have diluted the triolein and tested evaporation of the solvent (methanol was used to dissolve triolein) on the reaction occurring in the pyroprobe. The drying temperature was selected in such a way so as to be above the boiling point of the solvent. Based on this criterion, 80 °C was selected to be an optimum temperature. Then the time for drying was reduced from 300 s to 60 s. A solvent peak of the same abundance was seen with all the evaluated time 300 s, 240 s, 180 s, and 120 s. Only at 60 s was the abundance of the solvent peak was much higher when compared to other times. Thus, 120 s was selected as the optimum time for drying.

The triolein sample was prepared in several different concentrations (300 – 1000 ppm) in methanol. This sample was spiked on the quartz tube using a syringe, with and without derivatization agent TMAH, which was spiked on top of it. At all the concentrations with and without the derivatization agent, only oleic acid was seen (not shown). This could mean that there was not enough sample to show pyrolysis. For this reason, the undiluted sample was introduced directly on the quartz tube using a syringe tip.

When the sample was introduced using a syringe tip, a number of analytes (C_5-C_{10} and $C_{18:1}$ acids) were seen for the pyrolysis of triolein. However, a carryover was observed for several runs. The carryover was eliminated only after replacing the desorption trap. This suggests that introducing a sample with the syringe tip overloaded

the system capacity. Because of the capillary action, the sample might have gotten into the syringe and might have introduced more onto the quartz wool. Figure 18 shows the TIC and extracted ion chromatograms (EIC) (60 *m/z*, specific for underivatized acids) for the pyrolysis of high concentration of neat triolein sample without the derivatization agent. The smaller (unlabeled) peaks observed with ion 60 *m/z* were not confirmed as acids using NIST 05 spectral library, the data suggested these could be fragments from olefins occurring at high abundance.

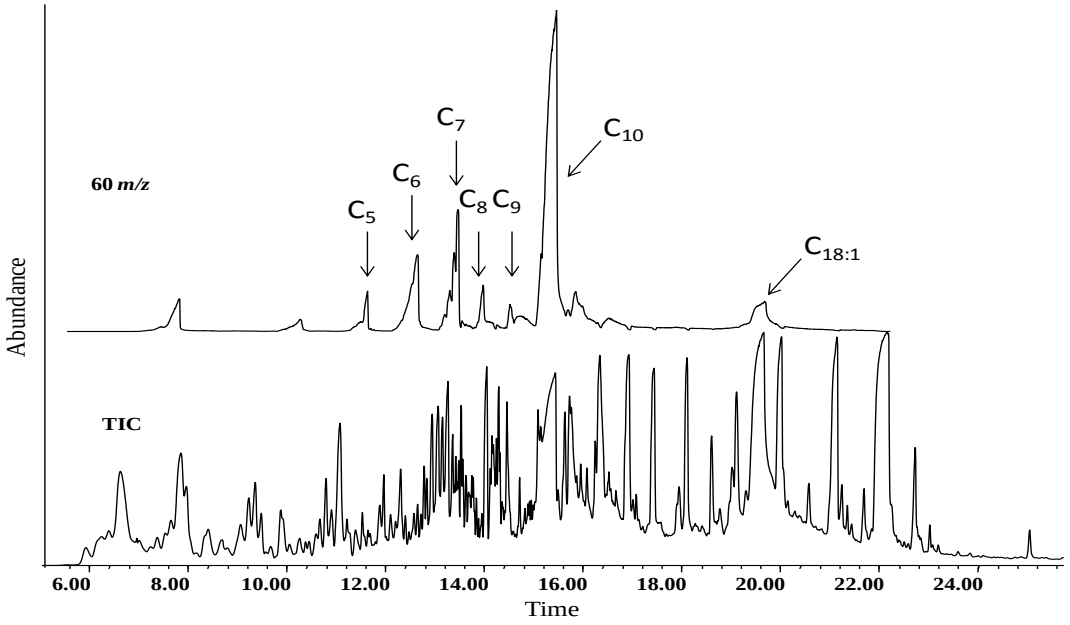

Figure 18. The chromatogram obtained using online Py-GC/MS shows the presence of C_{10} FA in pyrolyzed underivatized triolein is confirmed using EIC (60 *m/z*).

In order to get an appropriate amount of sample onto the quartz tube, the triolein sample was introduced using a plunger tip (from microsyringe). Several peaks were seen, with oleic acid being prominent. However, none of the other acids were observed possibly due broadness of peaks in underivatized form and thus reduced sensitivity of the

analysis. In order to increase sensitivity for the acid species, the derivatization agent, TMAH, was spiked on the quartz tube after the sample was spiked.

The acids were identified based on the analysis of derivatized standards direcnly injected into GC/MS, as shown in Figure 19 showing TIC and EIC for common ions of 74, 87 and 143 *m/z*. The pyroprobe temperature for pyrolysis was optimized by changing the temperature from 750 ℃ to 450 ℃. We started using higher temperatures first in order to avoid clogging of the sample in the transfer line. A minute amount of acids ($C_6 - C_{10}$, C_{16} and $C_{18:1}$) were seen at all the temperatures, as presented in Figure 20 for extracted ion of 87 *m/z*.

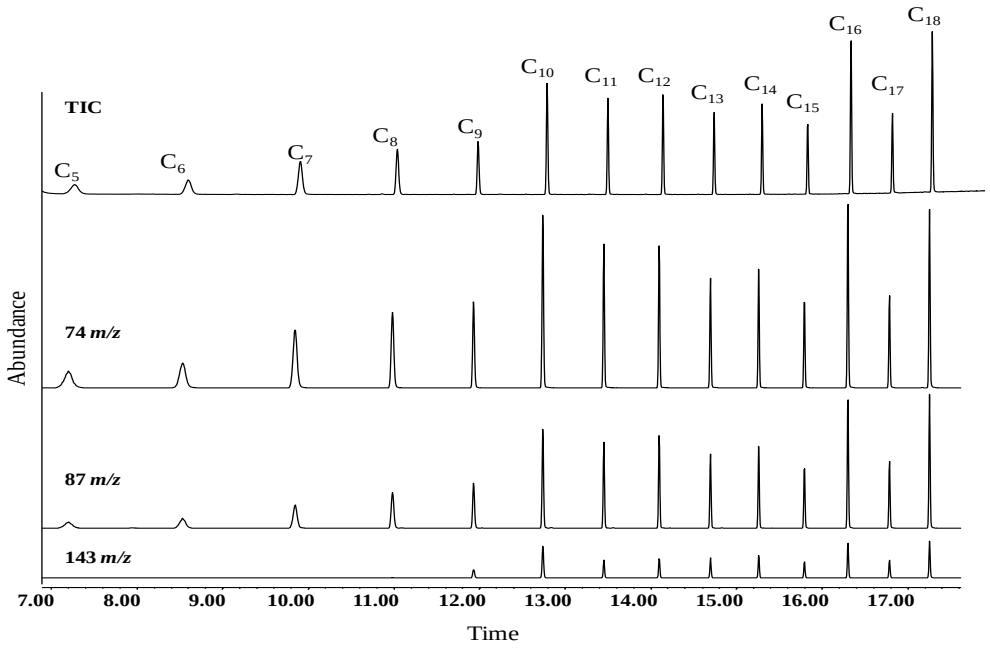

Figure 19. GC-MS chromatogram showing derivatized acid standards analyzed following direct injection using TIC and EIC (74, 87 and 143 *m/z*).

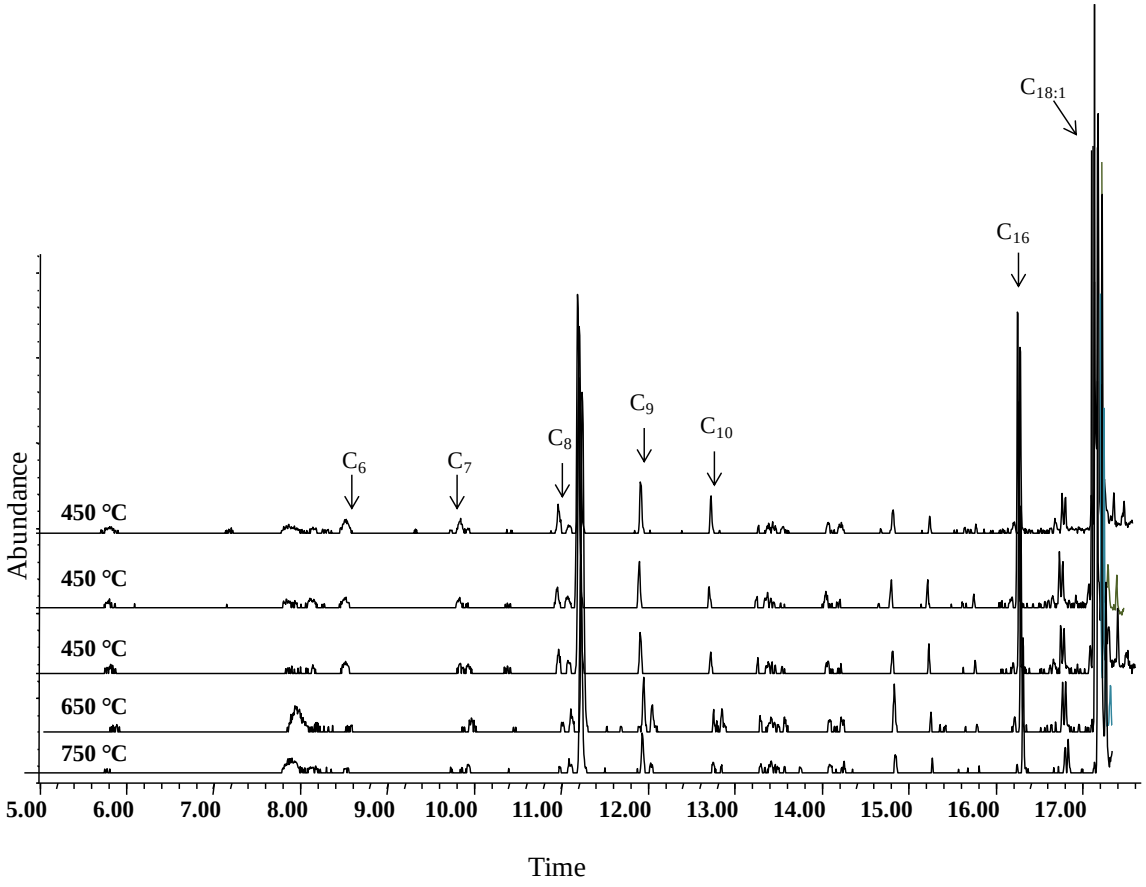

Figure 20. The chromatograms obtained using online Py-GC/MS with TMAH derivatization showing the presence of C_9 and C_{10} FAs in pyrolyzed triolein at different pyroprobe temperatures using EIC (87 *m/z*).

The results from the online Py-GC/MS support that the feedstocks which have high oleic acid (i.e., canola) will predominantly lead to the formation of C_9 and C_{10} FA via the mechanistic pathway proposed in Figure 10.

5. CONCLUSION

All feedstocks showed specific FA homology profiles depending on their initial FA composition; particularly, their double bond patterns. Crop oils with high linoleic acid content, i.e., soybean, cottonseed and corn oils, showed the C_7 FA as the preferred pyrolysis product (preferred C_7 path). Crop oils with high oleic acid content, i.e., canola and, particularly, high oleic canola oils, feature the C_9 and C_{10} FA as the major pyrolysis product (preferred C_9-C_{10} path). C_{18} is the only unsaturated FAs observed in significant amounts as they are uncracked. Acetic and propionic acids were also observed abundantly in the pyrolysis products of all crop oil pyrolysis patterns. Jojoba oil being a non-glycerol based feedstock demonstrated a similar homology profile as that of soybean and canola oils. Also, C_9-C_{10} paths were preferred as jojoba oil has a high amount of oleic acid. Cuphea oil has C_{10} as a major pyrolysis product as it contains a large amount of C_{10} FA in its original composition. In cuphea oil, several ketones were also seen, C_{19} being prominent. The position and a number of double bounds and FA chain length in different feedstocks affected the pyrolysis pattern. By performing pyrolysis of a model compound, triolein, it was proved that the species with high oleic acid content will follow predominantly the C_9-C_{10} path. While this work targeted pyrolyzed crop oils, the same mechanistic aspects will be applicable to any TG non-food oils, which may be used for industrial fuel production in the future.

6. APPENDICES

Appendix A

GC Chromatograms

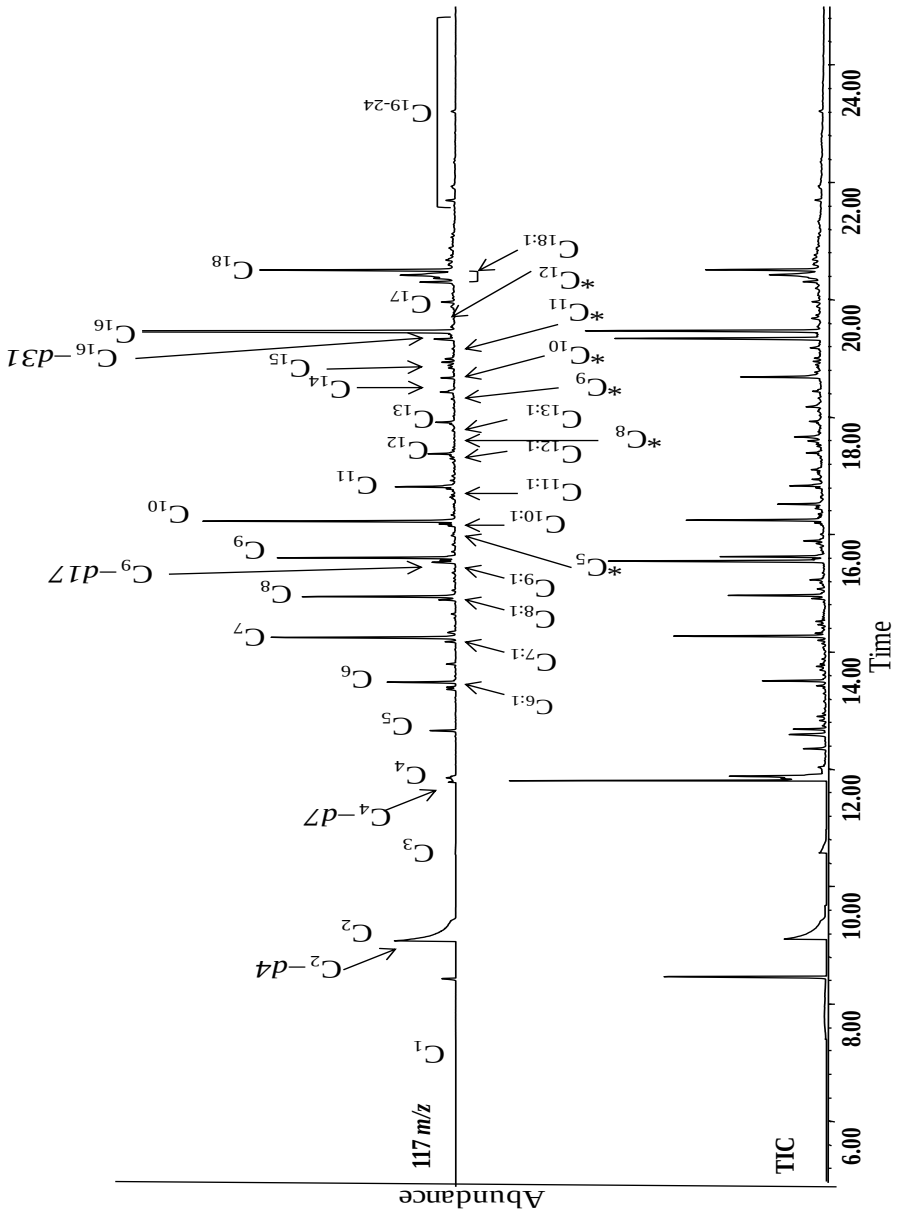

Figure 21. TIC and EIC of soybean OLP sample using ion (117 *m/z*). Chemical engineering label: ML-2011-10-05a-TTR corresponding to GC sequence: 13-0420 and label:23 AG13-1A (*d* deuterated sample, * dicarboxylic acids).

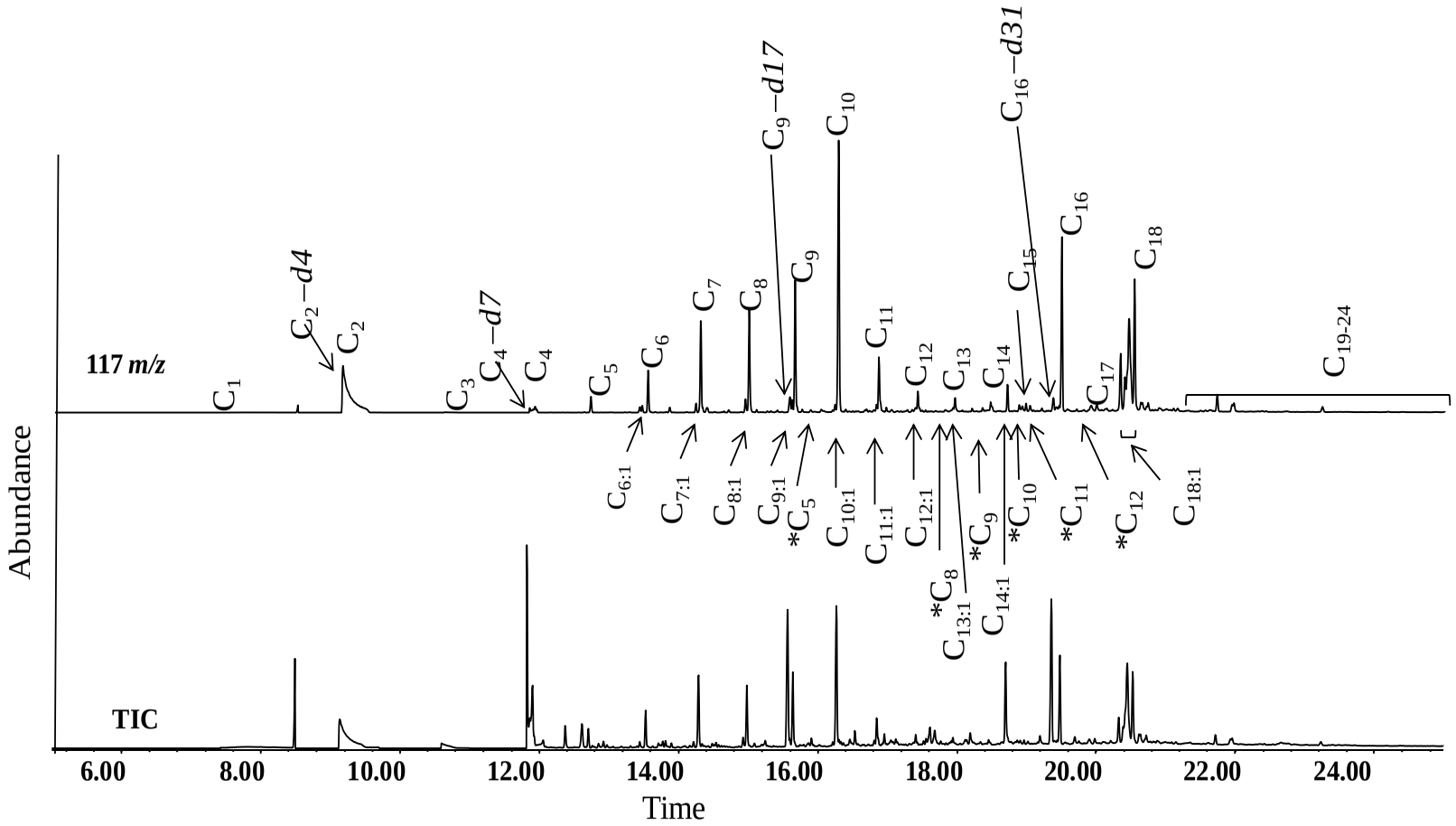

Figure 22. TIC and EIC of canola OLP sample using ion (117 *m/z*). Chemical engineering label: ML-2011-10-05e-TTR corresponding to GC sequence: 13-0420 and label:29 AG13-4A (*d* deuterated sample, * dicarboxylic acids).

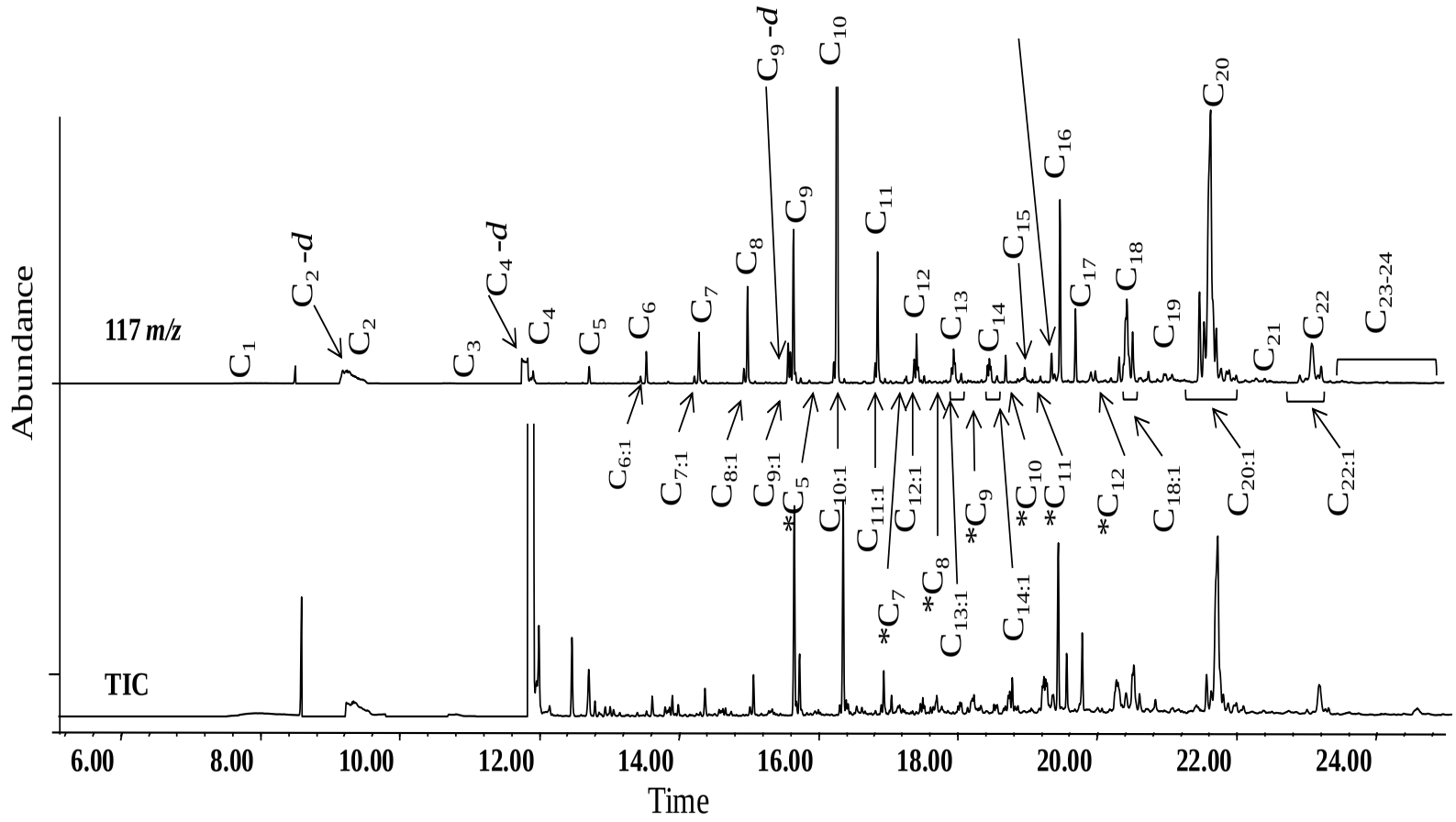

Figure 23. TIC and EIC of jojoba OLP sample using ion (117 *m/z*). Chemical engineering label: ML-2011-08-19p-PFR corresponding to GC sequence: 12-1029 and label:18 AG4-7 (*d* deuterated sample, * dicarboxylic acids).

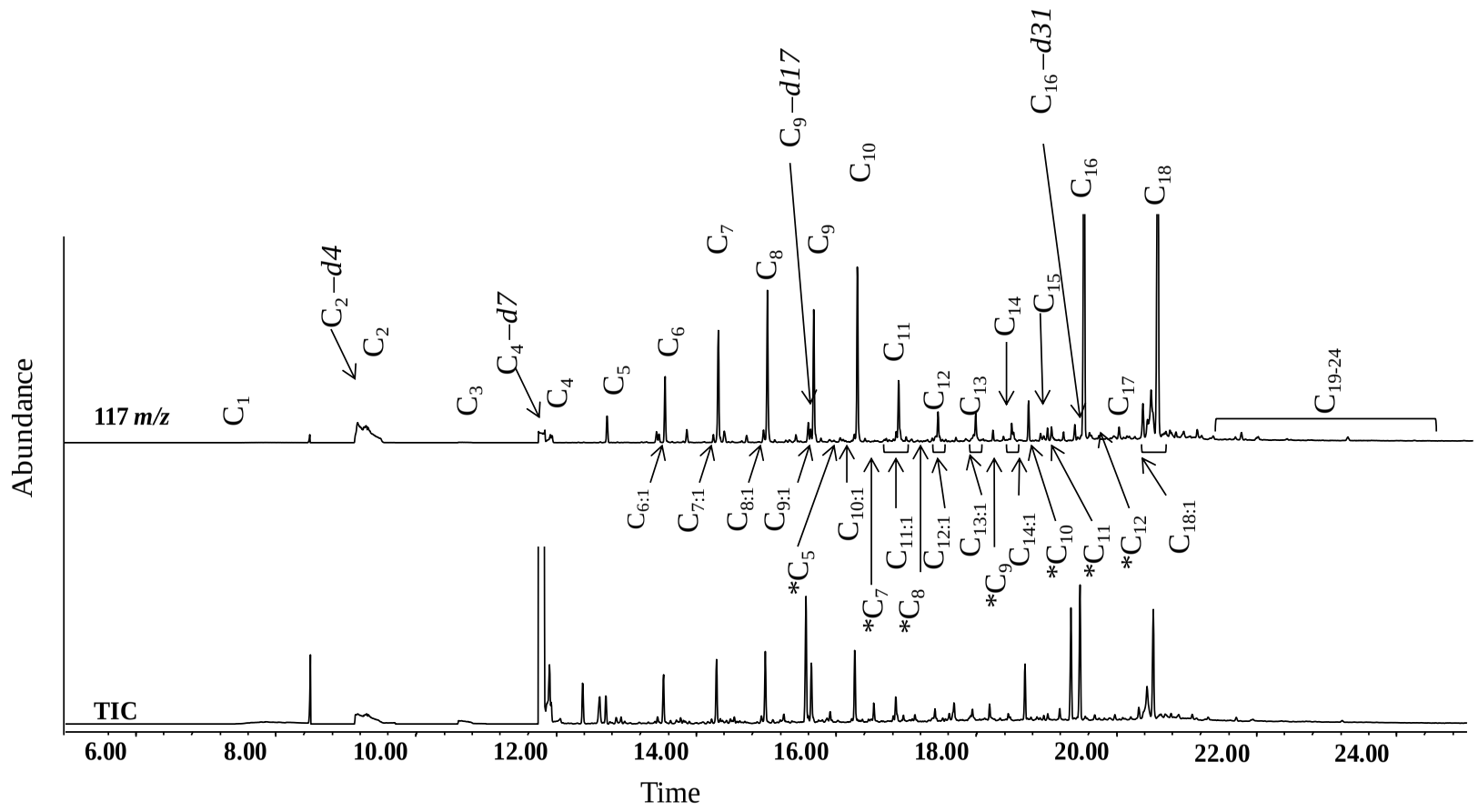

Figure 24. TIC and EIC of linseed OLP sample using ion (117 *m/z*). Chemical engineering label: ML-2011-08-20g-PFR corresponding to GC sequence: 12-1029 and label:19 AG4-10A (*d* deuterated sample, * dicarboxylic acids).

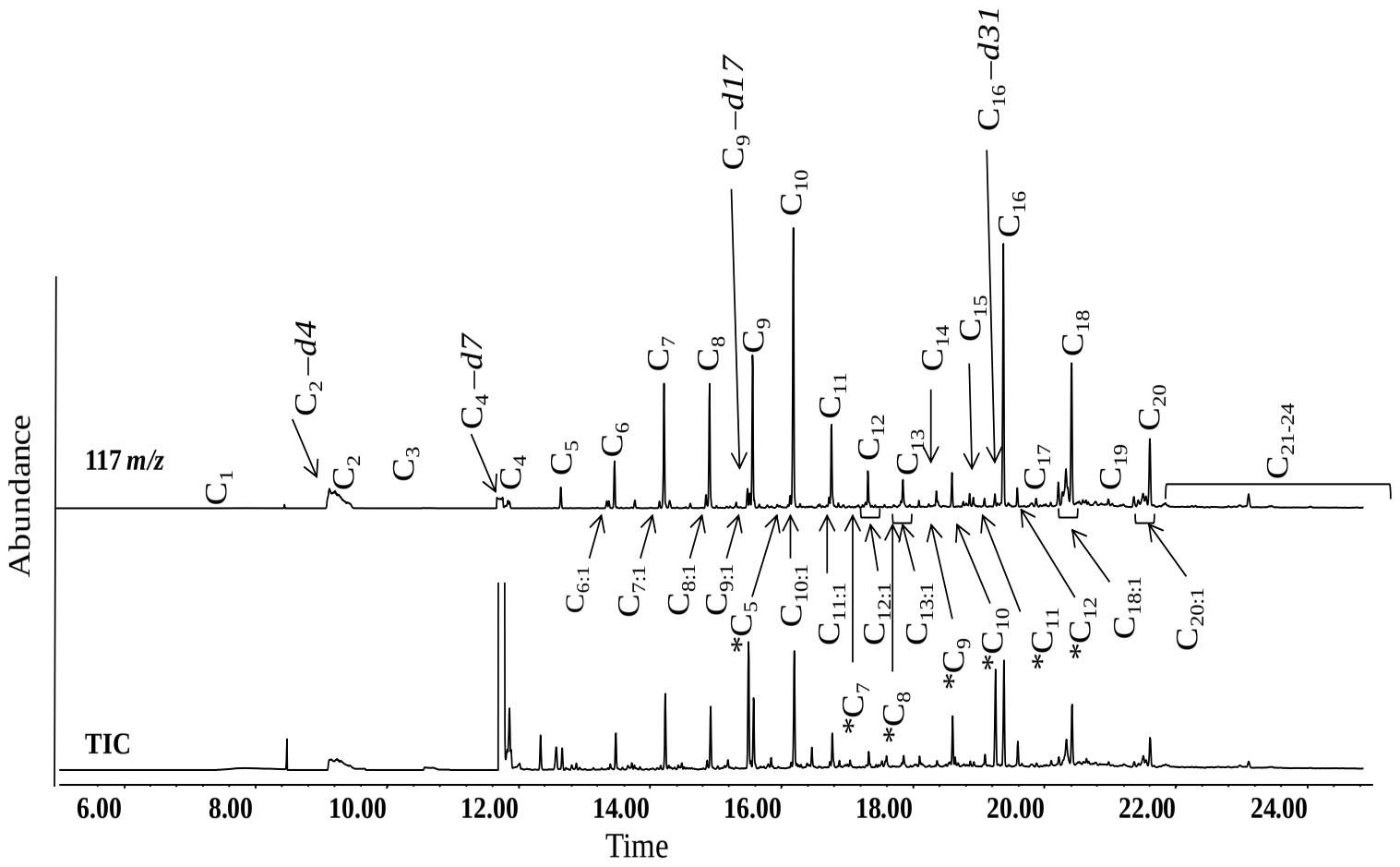

Figure 25. TIC and EIC of camelina OLP sample using ion (117 *m/z*). Chemical engineering label: ML-2011-08-20m-PFR corresponding to GC sequence: 12-1029 and label:41 AG4-13 (*d* deuterated sample, * dicarboxylic acids).

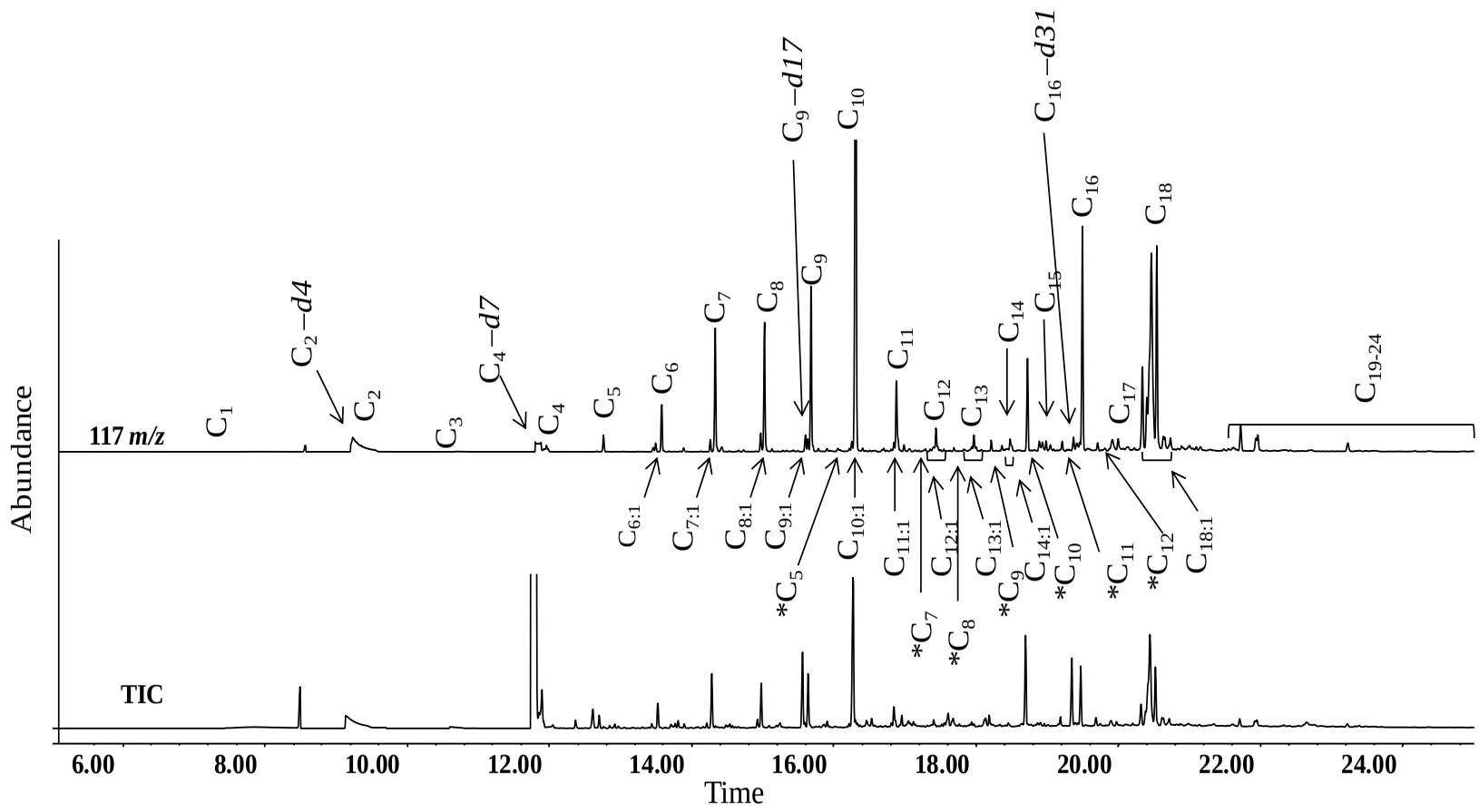

Figure 26. TIC and EIC of high oleic (75 %) canola oil OLP sample using ion (117 *m/z*). Chemical engineering label: ML-2011-08-19m-PFR corresponding to GC sequence: 12-1102 and label:19 AG6-7 (*d* deuterated sample, * dicarboxylic acids).

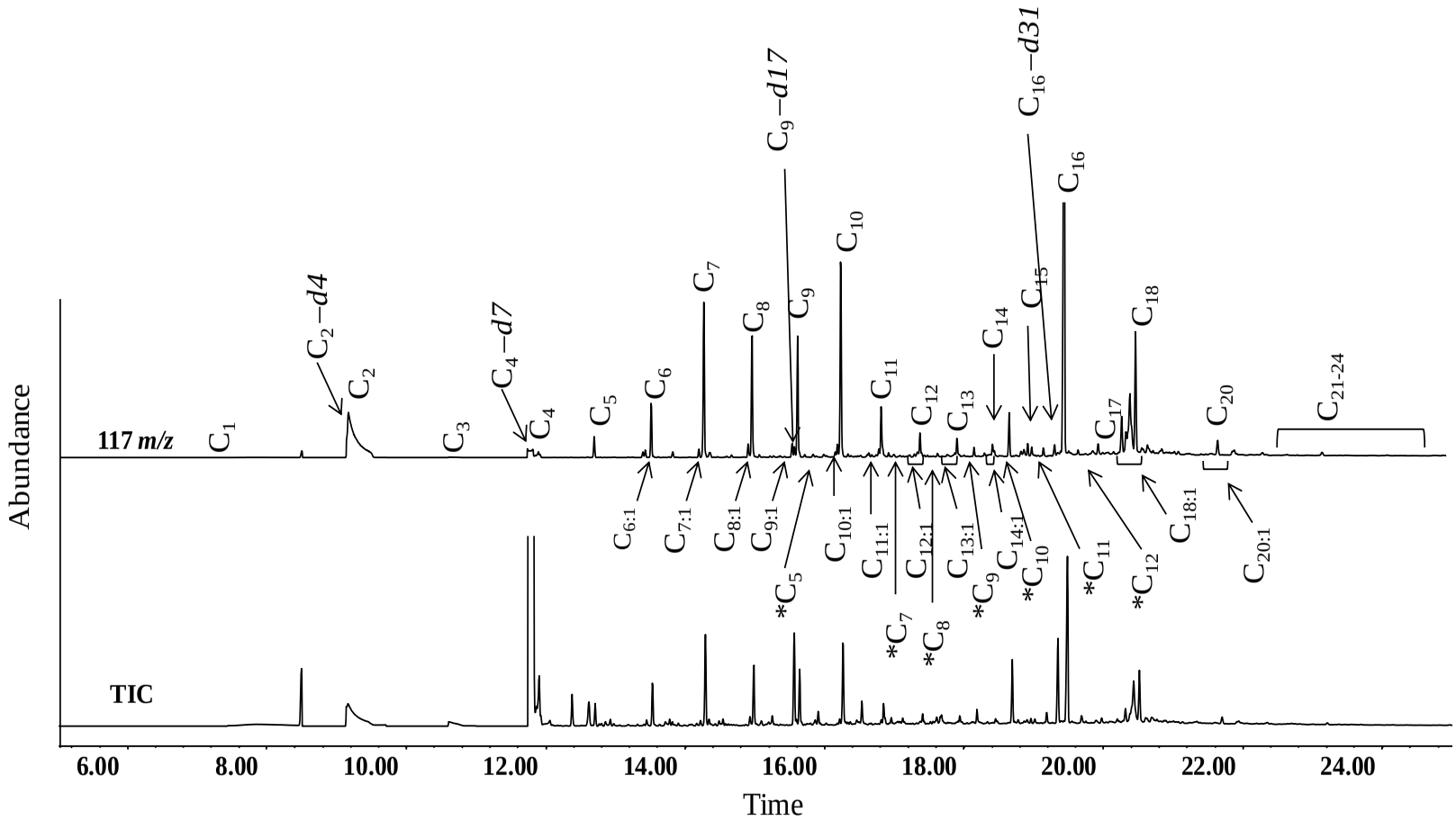

Figure 27. TIC and EIC of corn OLP sample using ion (117 *m/z*). Chemical engineering label: ML-2011-08-20a-PFR corresponding to GC sequence: 12-1102 and label:40 AG6-10A (*d* deuterated sample, * dicarboxylic acids).

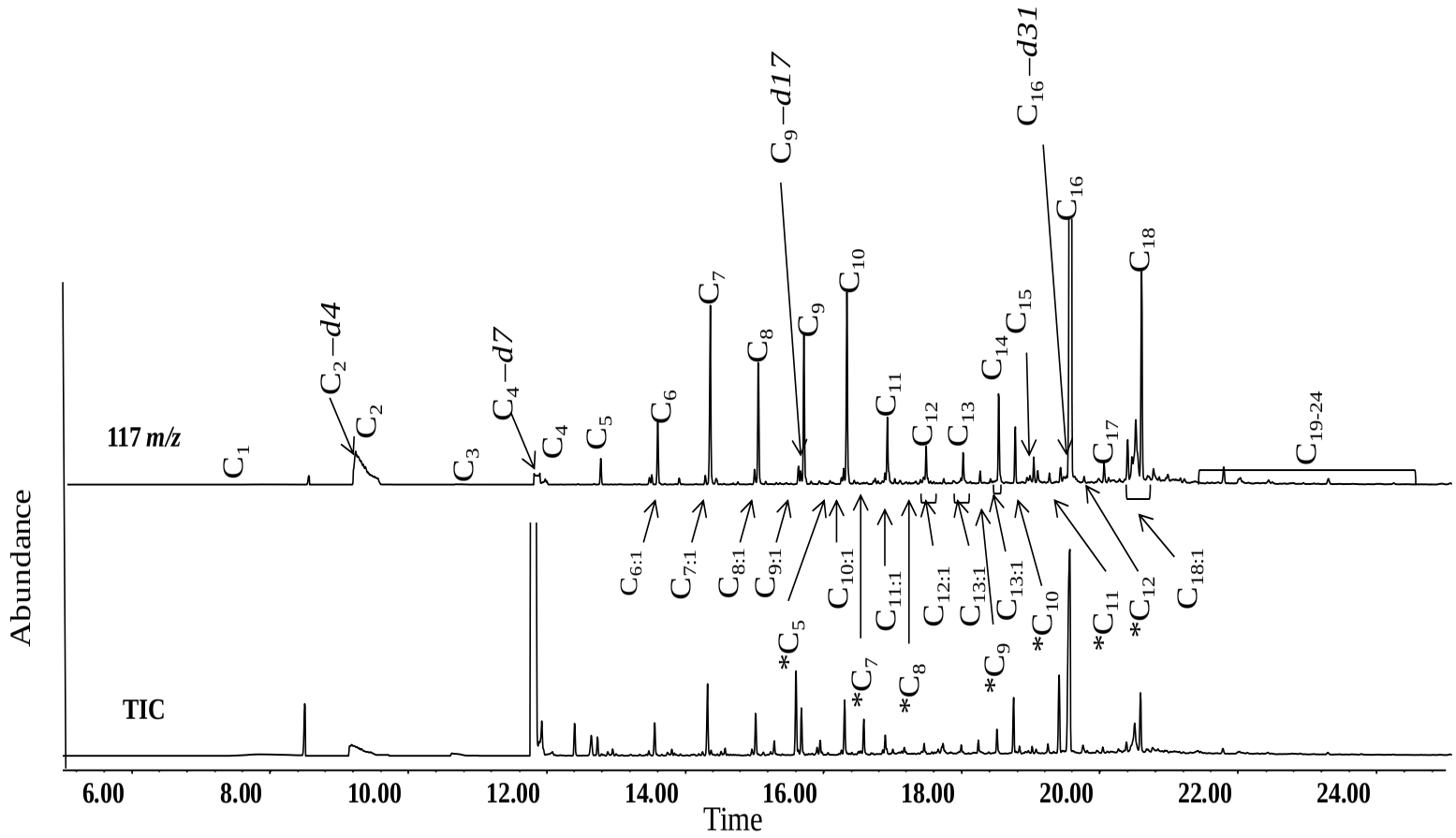

Figure 28. TIC and EIC of cotton OLP sample using ion (117 *m/z*). Chemical engineering label: ML-2011-08-20d-PFR corresponding to GC sequence: 12-1102 and label:59 AG6-13A (*d* deuterated sample, * dicarboxylic

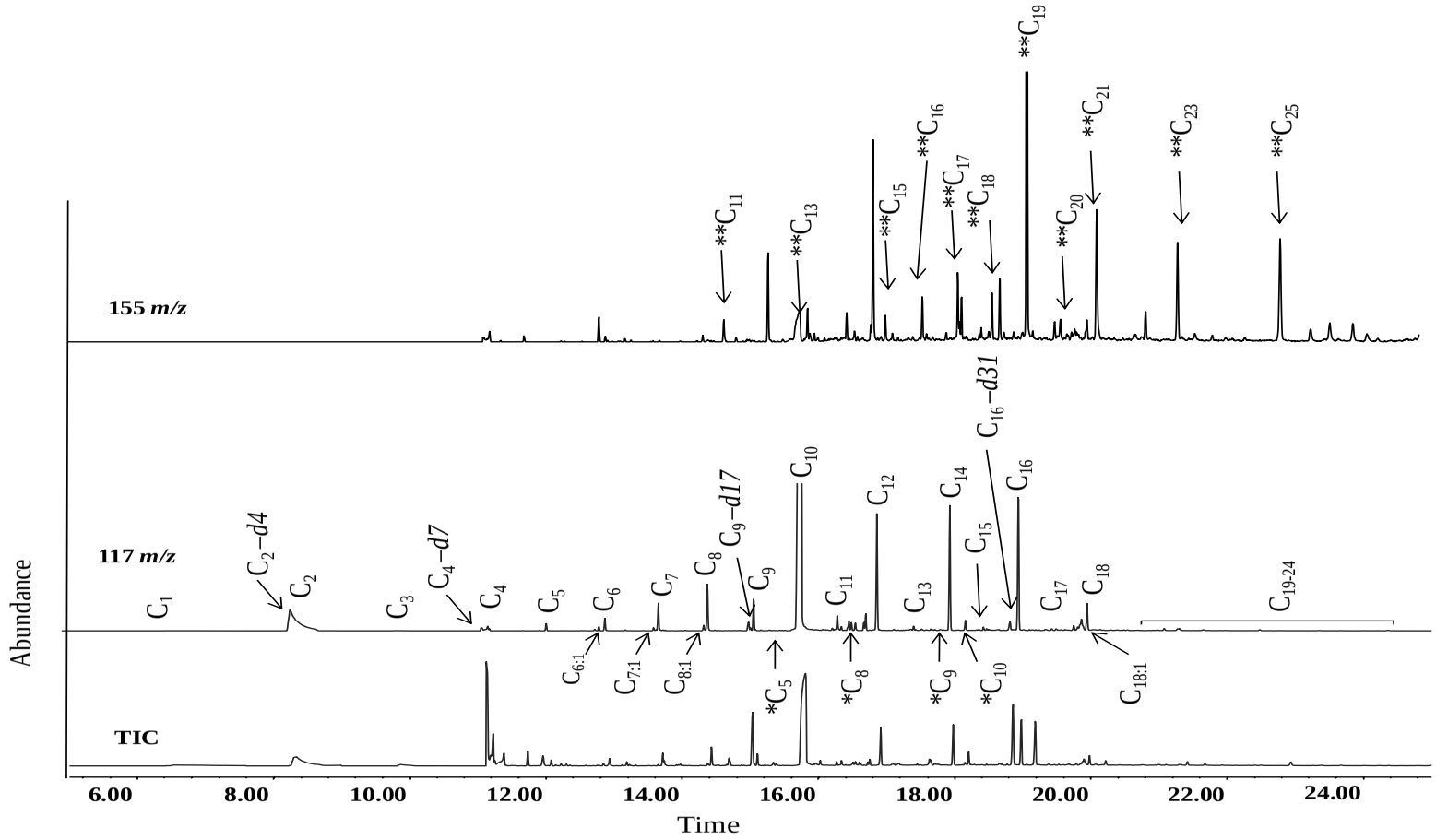

Figure 29. TIC and EIC of cuphea OLP sample using ions (117, 155 *m/z*). Chemical engineering label: ML-2011-08-20p-PFR corresponding to GC sequence: 13-0526_AG and label: 21 AG16-9 (*d* deuterated sample, * dicarboxylic acids, ** ketones).

Appendix B

Summary of Data in mol %

Table 7. Summary (mol %) of saturated carboxylic acids of soybean, cotton, corn and canola OLPs with their standard deviation (n=3)

	Soybean		Canola		Cotton		Corn	
Carbon #	Avg	Std	Avg	Std	Avg	Std	Avg	Std
1	3.727	0.356	2.459	0.275	3.223	0.129	3.929	0.151
2	13.025	0.879	11.162	0.370	14.122	0.835	16.680	2.140
3	8.850	0.994	5.727	0.085	6.650	0.287	7.902	0.219
4	3.591	0.251	3.358	0.170	2.493	0.142	2.909	0.104
5	2.951	0.211	2.451	0.094	3.230	0.076	3.727	0.133
6	4.423	0.145	4.800	0.093	4.661	0.148	5.477	0.180
7	9.706	0.379	8.392	0.136	8.694	0.323	10.016	0.497
8	5.383	0.159	6.056	0.155	4.926	0.196	5.790	0.267
9	5.150	0.207	7.217	0.271	4.300	0.116	5.055	0.277
10	6.794	0.194	16.420	0.313	4.625	0.163	6.659	0.339
11	1.771	0.143	1.627	0.094	1.528	0.029	1.788	0.073
12	0.995	0.132	0.738	0.031	0.966	0.020	1.053	0.033
13	0.805	0.057	0.547	0.017	0.919	0.026	1.006	0.032
14	0.720	0.110	0.467	0.026	1.526	0.031	0.827	0.025
15	0.234	0.011	0.153	0.011	0.376	0.014	0.297	0.016
16	13.706	0.331	4.736	0.152	26.288	1.249	13.140	0.644
17	0.209	0.010	0.134	0.009	0.167	0.007	0.139	0.006
18	5.651	0.378	4.150	0.089	2.818	0.070	2.681	0.080
19	0.042	0.016	0.102	0.003	0.089	0.003	0.087	0.004
20	0.293	0.030	0.562	0.023	0.331	0.016	0.462	0.030
21	0.023	0.004	0.079	0.002	0.055	0.003	0.052	0.002
22	0.219	0.034	0.281	0.016	0.177	0.009	0.164	0.010
23	0.041	0.009	0.058	0.003	0.067	0.004	0.056	0.003
24	0.087	0.017	0.159	0.010	1.051	0.039	1.239	0.040
Total	88.396	1.612	81.835	0.537	93.282	0.228	91.134	0.407

Table 8. Summary (mol %) of saturated carboxylic acids of camelina, linseed, cuphea, high oleic (75 %) canola oil (HOCO) and jojoba OLPs with their standard deviation (n=3)

	Camelina		Linseed		Cuphea		HOCO		Jojoba	
Carbon #	Avg	Std	Avg	Std	Avg	Std	Avg	Std	Avg	Std
1	3.966	0.252	2.809	0.202	0.059	0.007	2.123	0.075	2.571	0.122
2	11.468	0.893	14.336	0.656	6.081	0.517	7.992	0.338	4.834	0.317
3	7.536	0.146	9.784	0.914	0.860	0.067	5.423	0.511	6.016	0.369
4	5.129	0.523	7.031	0.270	0.671	0.045	1.495	0.027	2.153	0.082
5	3.981	0.191	4.887	0.219	0.514	0.052	1.719	0.054	2.396	0.120
6	4.801	0.133	5.835	0.578	0.529	0.063	3.290	0.114	2.475	0.032
7	7.263	0.365	8.397	0.650	0.799	0.086	5.692	0.231	2.429	0.074
8	6.031	0.369	7.183	0.357	1.262	0.117	4.679	0.124	2.469	0.052
9	5.934	0.182	6.293	0.322	0.645	0.095	5.591	0.166	3.438	0.047
10	7.889	0.904	5.837	0.181	79.988	1.596	30.707	0.660	10.497	0.146
11	2.579	0.026	2.130	0.044	0.208	0.021	2.013	0.011	2.188	0.033
12	1.282	0.032	1.226	0.025	2.200	0.163	0.911	0.022	1.153	0.024
13	1.204	0.065	1.129	0.040	0.043	0.005	0.785	0.027	1.051	0.037
14	0.920	0.053	0.796	0.029	1.948	0.135	0.929	0.039	0.767	0.027
15	0.324	0.019	0.264	0.009	0.039	0.003	0.171	0.004	0.173	0.006
16	6.822	0.359	7.761	0.474	2.223	0.175	4.507	0.029	2.853	0.314
17	0.132	0.010	0.137	0.005	0.017	0.003	0.105	0.005	0.070	0.001
18	3.003	0.100	5.363	0.254	0.254	0.030	3.300	0.030	1.266	0.129
19	0.146	0.003	0.113	0.003	0.014	0.003	0.080	0.004	0.111	0.006
20	0.341	0.033	0.222	0.006	0.043	0.002	0.570	0.019	0.904	0.071
21	0.076	0.003	0.059	0.003	0.007	0.001	0.041	0.002	0.095	0.005
22	0.559	0.031	0.198	0.012	0.033	0.001	0.278	0.013	0.445	0.035
23	0.079	0.006	0.075	0.003	0.011	0.000	0.052	0.003	0.076	0.001
24	0.000	0.000	0.000	0.000	0.020	0.001	1.401	0.082	1.338	0.052
Total	81.466	0.691	91.866	0.255	98.468	0.022	83.856	0.322	51.768	1.721

Table 9. Summary (mol %) of unsaturated carboxylic acids of soybean, cotton, corn and canola OLPs with their standard deviation (n=3)

	Soybean		Canola		Cotton		Corn	
carbon #	Avg	Std	Avg	Std	Avg	Std	Avg	Std
6	0.094	0.005	0.109	0.007	0.167	0.006	0.193	0.007
7	0.048	0.004	0.071	0.005	0.115	0.004	0.133	0.006
8	0.218	0.010	0.230	0.011	0.248	0.009	0.299	0.014
9	0.117	0.003	0.124	0.019	0.131	0.005	0.152	0.010
10	0.091	0.003	0.057	0.005	0.129	0.008	0.141	0.008
11	0.120	0.004	0.114	0.009	0.140	0.005	0.158	0.010
12	0.083	0.015	0.067	0.005	0.169	0.004	0.189	0.003
13	0.058	0.005	0.059	0.006	0.116	0.005	0.122	0.014
14	0.032	0.004	0.020	0.002	0.083	0.005	0.090	0.004
18	4.242	0.368	7.831	0.179	4.648	0.178	6.293	0.372
20	0.000	0.000	8.681	0.219	0.089	0.009	0.116	0.011
22	0.000	0.000	0.000	0.000	0.000	0.000	0.000	0.000
Total	5.102	0.363	0.506	0.053	6.037	0.202	7.886	0.400

Table 10. Summary (mol %) of unsaturated carboxylic acids of camelina, linseed, cuphea, high oleic (75 %) canola oil (HOCO) and jojoba OLPs with their standard deviation (n=3)

	Camelina		Linseed		Cuphea		HOCO		Jojoba	
carbon #	Avg	Std	Avg	Std	Avg	Std	Avg	Std	Avg	Std
6	0.184	0.001	0.205	0.015	0.034	0.003	0.175	0.004	0.129	0.009
7	0.117	0.012	0.168	0.009	0.028	0.005	0.124	0.002	0.083	0.036
8	0.294	0.013	0.311	0.014	0.050	0.004	0.295	0.004	0.159	0.006
9	0.194	0.007	0.179	0.011			0.142	0.006	0.221	0.017
10	0.151	0.010	0.126	0.007			0.111	0.009	0.180	0.010
11	0.190	0.001	0.466	0.037			0.143	0.003	0.174	0.005
12	0.231	0.007	0.236	0.011			0.165	0.011	0.357	0.011
13	0.252	0.015	0.235	0.010			0.132	0.027	0.310	0.055
14	0.141	0.023	0.090	0.007			0.071	0.002	0.284	0.009
18	4.843	0.175	5.488	0.224	0.463	0.027	13.313	0.304	5.960	1.055
20	8.701	0.530	0.084	0.006			0.339	0.003	26.972	1.447
22									7.074	0.120
Total	15.298	0.706	7.586	0.263	0.575	0.039	15.009	0.308	41.902	1.819

Table 11. Summary (mol %) of di-carboxylic acids of soybean, cotton, corn and canola OLPs with their standard deviation (n=3)

	Soybean		Canola		Cotton		Corn	
carbon #	Avg	Std	Avg	Std	Avg	Std	Avg	Std
5	0.896	0.091	0.506	0.053	0.628	0.192	0.920	0.257
7	0.084	0.021	0.134	0.015	0.070	0.009	0.084	0.008
8	0.251	0.108	0.327	0.063	0.292	0.014	0.338	0.013
9	1.308	0.488	1.422	0.244	1.311	0.047	1.500	0.085
10	3.207	0.607	4.450	0.225	2.845	0.071	3.480	0.183
11	0.492	0.082	1.513	0.244	1.303	0.062	1.208	0.031
12	0.264	0.109	1.132	0.178	0.681	0.031	0.980	0.028
Total	6.503	1.399	9.484	0.664	7.130	0.257	8.510	0.411

Table 12. Summary (mol %) of di-carboxylic acids of camelina, linseed, cuphea, high oleic (75 %) canola oil (HOCO) and jojoba OLPs with their standard deviation (n=3)

	Camelina		Linseed		Cuphea		HOCO		Jojoba	
carbon #	Avg	Std	Avg	Std	Avg	Std	Avg	Std	Avg	Std
5	0.351	0.039	0.000	0.000	0.138	0.012	0.363	0.039	0.031	0.009
7	0.072	0.000	0.072	0.021	0.023	0.001	0.062	0.004	0.016	0.001
8	0.274	0.001	0.351	0.051	0.055	0.001	0.243	0.013	0.037	0.003
9	1.190	0.041	1.507	0.095	0.175	0.010	1.388	0.009	0.116	0.005
10	2.537	0.040	3.305	0.290			5.960	0.324	1.384	0.130
11	1.577	0.059	1.390	0.057	0.567	0.013	1.376	0.036	0.463	0.032
12	3.236	0.195	0.547	0.028			1.135	0.026	6.330	0.467
Total	9.235	0.330	7.174	0.407	0.957	0.034	10.528	0.300	8.378	0.457

Table 13. Summary (mol %) of ketones of cuphea OLP with their standard deviation (n=3)

Table B-6.

Carbon #	Avg	Std
11	15.82	1.29
12	2.88	0.15
13	0.67	0.05
14	2.48	0.09
15	1.44	0.03
16	2.52	0.11
17	2.31	0.16
18	1.66	0.12
19	68.95	1.89
21	0.45	0.02
22	0.03	0.00
23	0.37	0.01
25	0.40	0.01

Ketones were found only in cuphea oil

APPENDIX C

Calibration Data for the Standards Used

Table 14. Calibration data for monosaturated carboxylic acids (C_1-C_3)

	Formic acid, TMS ester			Acetic acid, TMS ester			Propanoic acid, TMS ester		
	Area / Area IS	Mass [µg/mL]	Area	Area / Area IS	Mass [µg/mL]	Area	Area / Area IS	Mass [µg/mL]	Area
Std G	0.04	0.56	255937	0.03	0.58	211170	0.02	0.42	147695
	0.04	0.56	272690	0.03	0.58	235620	0.02	0.42	172715
Std F	0.06	1.67	386834	0.05	1.75	332207	0.03	1.25	221467
	0.05	1.67	411096	0.05	1.75	387300	0.03	1.25	262403
Std E	0.10	5.00	697410	0.10	5.25	655584	0.06	3.75	430261
	0.10	5.00	808107	0.10	5.25	755206	0.07	3.75	508807
Std D	0.27	14.99	1801310	0.25	15.74	1721961	0.17	11.26	1136284
	0.27	14.99	1899860	0.25	15.74	1751450	0.16	11.26	1148418
Std C	0.69	44.98	4773028	0.65	47.23	4496798	0.44	33.78	3073860
	0.70	44.98	4753675	0.65	47.23	4408005	0.44	33.78	2983414
Std B	1.81	134.94	11591133	1.68	141.70	10772736	1.16	101.34	7444587
	1.86	134.94	14427015	1.68	141.70	13055785	1.15	101.34	8918946
Std A	5.28	404.82	35956616	4.78	425.10	32556229	3.39	304.03	23119315
	5.35	404.82	40403436	4.76	425.10	35954417	3.36	304.03	25384893
LOQ	**UCL**	0.01	5.31		0.01	4.77		0.01	3.38
m	**B**	0.015	0.033		0.012	0.048		0.011	0.030
STD for m	**STD for b**	0.000	0.004		0.000	0.010		0.000	0.006
R^2	**STD for y**	0.999	0.009		0.998	0.029		0.998	0.018
F	**df**	6883	8		4775	10		6107	10

Std A to Std G represent different concentrations, Std A being the highest concentration. LOQ=Limit of Quantification, UCL=Upper calibration limit (for highest three concentrations), b=intercept, m=slope, R^2= The coefficient of determination. F= F statistic, df=degrees of freedom

Table 15. Calibration data for monosaturated carboxylic acids (C_4-C_6)

	Butanoic acid, TMS ester			Pentanoic acid, TMS ester			Hexanoic acid, TMS ester		
	Area / Area IS	Mass [µg/mL]	Area	Area / Area IS	Mass [µg/mL]	Area	Area / Area IS	Mass [µg/mL]	Area
Std G	0.03	0.57	177133	0.03	0.59	187403	0.03	0.57	173600
	0.03	0.57	206361	0.03	0.59	211180	0.03	0.57	193773
Std F	0.04	1.70	276753	0.04	1.78	280265	0.04	1.71	253713
	0.04	1.70	314616	0.04	1.78	315738	0.04	1.71	284863
Std E	0.08	5.11	540724	0.08	5.33	558176	0.07	5.14	499900
	0.08	5.11	601895	0.08	5.33	629289	0.07	5.14	576582
Std D	0.21	15.34	1432056	0.22	15.99	1489337	0.20	15.43	1364352
	0.22	15.34	1523161	0.21	15.99	1491713	0.19	15.43	1335358
Std C	0.58	46.01	4004664	0.58	47.97	4049251	0.53	46.30	3703884
	0.59	46.01	4033666	0.57	47.97	3840728	0.52	46.30	3512969
Std B	1.54	138.04	9867590	1.45	143.91	9315694	1.36	138.91	8716803
	1.48	138.04	11464460	1.43	143.91	11074501	1.31	138.91	10144860
Std A	3.58	414.11	24384816	3.47	431.74	23647154	3.23	416.73	21975293
	3.54	414.11	26711681	3.40	431.74	25656732	3.16	416.73	23864027
LOQ	**UCL**	0.01	3.56		0.01	3.43		0.00	3.19
m	**b**	0.012	0.020		0.012	0.023		0.011	0.021
STD for m	**STD for b**	0.000	0.003		0.000	0.003		0.000	0.002
R^2	**STD for y**	0.999	0.007		0.999	0.007		0.999	0.006
F	**df**	9930	8		9049	8		9640	8

Std A to Std G represent different concentrations, Std A being the highest concentration. LOQ=Limit of Quantification, UCL=Upper calibration limit (for highest three concentrations), b=intercept, m=slope, R^2= The coefficient of determination. F= F statistic, df=degrees of freedom

Table 16. Calibration data for monosaturated carboxylic acids (C_7-C_9)

	Heptanoic acid, TMS ester			Octanoic acid, TMS ester			Nonanoic acid, TMS ester		
	Area / Area IS	Mass [µg/mL]	Area	Area / Area IS	Mass [µg/mL]	Area	Area / Area IS	Mass [µg/mL]	Area
Std G	0.04	0.75	250972	0.03	0.60	180083	0.02	0.53	140362
	0.04	0.75	289058	0.03	0.60	212608	0.02	0.53	164848
Std F	0.05	2.26	356760	0.04	1.81	260287	0.03	1.58	203530
	0.05	2.26	408557	0.04	1.81	296391	0.03	1.58	242999
Std E	0.10	6.78	697561	0.08	5.43	520563	0.06	4.73	402782
	0.10	6.78	785789	0.08	5.43	594413	0.06	4.73	459327
Std D	0.28	20.35	1882774	0.22	16.30	1467138	0.17	14.20	1126661
	0.26	20.35	1831447	0.20	16.30	1408283	0.15	14.20	1066165
Std C	0.73	61.06	5102041	0.58	48.91	4065134	0.45	42.60	3148815
	0.71	61.06	4799405	0.57	48.91	3857466	0.44	42.60	2975233
Std B	1.78	183.18	11453299	1.51	146.73	9698884	1.22	127.81	7853581
	1.75	183.18	13547000	1.47	146.73	11375761	1.18	127.81	9163474
Std A	4.03	549.55	27468265	3.61	440.20	24592519	3.08	383.42	21007704
	3.91	549.55	29532967	3.51	440.20	26479844	2.98	383.42	22545549
LOQ	**UCL**	0.01	3.97		0.01	3.56		0.01	3.03
m	**b**	0.011	0.030		0.010	0.036		0.010	0.015
STD for m	**STD for b**	0.000	0.004		0.000	0.010		0.000	0.002
R^2	**STD for y**	0.999	0.009		0.997	0.029		0.999	0.005
F	**df**	7395	8		3923	10		9211	8

Std A to Std G represent different concentrations, Std A being the highest concentration. LOQ=Limit of Quantification, UCL=Upper calibration limit (for highest three concentrations), b=intercept, m=slope, R^2= The coefficient of determination. F= F statistic, df=degrees of freedom

Table 17. Calibration data for monosaturated carboxylic acids (C_{10}-C_{12})

	Decanoic acid, TMS ester			Undecanoic acid, TMS ester			Dodecanoic acid, TMS ester		
	Area / Area IS	Mass [µg/mL]	Area	Area / Area IS	Mass [µg/mL]	Area	Area / Area IS	Mass [µg/mL]	Area
Std G	0.03	0.80	219298	0.01	0.43	94219	0.01	0.42	91884
	0.04	0.80	268596	0.02	0.43	118897	0.02	0.42	122488
Std F	0.05	2.41	318044	0.02	1.28	137717	0.02	1.25	127643
	0.05	2.41	381164	0.02	1.28	171461	0.02	1.25	166414
Std E	0.09	7.23	626354	0.04	3.83	288059	0.04	3.74	267058
	0.10	7.23	742663	0.04	3.83	337439	0.04	3.74	329285
Std D	0.27	21.68	1826273	0.12	11.48	842786	0.12	11.21	832351
	0.25	21.68	1772186	0.12	11.48	826776	0.12	11.21	815687
Std C	0.74	65.05	5175247	0.36	34.43	2524634	0.36	33.64	2505240
	0.72	65.05	4909603	0.35	34.43	2357456	0.34	33.64	2339882
Std B	1.95	195.14	12495906	1.01	103.28	6476388	1.02	100.93	6518465
	1.90	195.14	14717323	0.99	103.28	7711219	1.01	100.93	7839832
Std A	4.59	585.43	31258328	2.78	309.84	18913678	2.82	302.78	19238026
	4.47	585.43	33735984	2.72	309.84	20585319	2.79	302.78	21098078
LOQ	**UCL**	0.02	4.53		0.01	2.75		0.02	2.81
m	**b**	0.007	0.253		0.009	0.028		0.009	0.024
STD for m	**STD for b**	0.000	0.081		0.000	0.010		0.000	0.009
R^2	**STD for y**	0.993	0.165		0.999	0.032		0.999	0.028
F	**df**	802	6		11686	12		16055	12

Std A to Std G represent different concentrations, Std A being the highest concentration. LOQ=Limit of Quantification, UCL=Upper calibration limit (for highest three concentrations), b=intercept, m=slope, R^2= The coefficient of determination. F= F statistic, df=degrees of freedom

Table 18. Calibration data for monosaturated carboxylic acids (C_{13}-C_{15})

	Tridecanoic acid, TMS ester			Tetradecanoic acid, TMS ester			Pentadecanoic acid, TMS ester		
	Area / Area IS	Mass [µg/mL]	Area	Area / Area IS	Mass [µg/mL]	Area	Area / Area IS	Mass [µg/mL]	Area
Std G	0.01	0.35	64124	0.01	0.35	62530	0.01	0.32	51715
	0.01	0.35	91705	0.01	0.35	100060	0.01	0.32	82309
Std F	0.01	1.04	96057	0.01	1.06	96597	0.01	0.96	73231
	0.02	1.04	123636	0.02	1.06	137723	0.02	0.96	114188
Std E	0.03	3.11	207703	0.03	3.19	200598	0.02	2.89	165610
	0.03	3.11	259418	0.03	3.19	268499	0.03	2.89	222937
Std D	0.09	9.32	626874	0.10	9.56	644277	0.08	8.68	552486
	0.09	9.32	627375	0.09	9.56	637213	0.08	8.68	551436
Std C	0.28	27.95	1946625	0.29	28.69	2051542	0.25	26.05	1734084
	0.27	27.95	1819228	0.29	28.69	1936343	0.24	26.05	1637723
Std B	0.80	83.85	5128752	0.86	86.07	5528661	0.74	78.16	4729876
	0.79	83.85	6136015	0.85	86.07	6598299	0.74	78.16	5738724
Std A	2.35	251.56	16035072	2.59	258.20	17636079	2.31	234.49	15729320
	2.29	251.56	17317390	2.53	258.20	19140226	2.24	234.49	16903997
LOQ	**UCL**	0.02	2.32		0.03	2.56		0.02	2.27
m	**b**	0.009	0.009		0.010	0.004		0.010	-0.002
STD for m	**STD for b**	0.000	0.005		0.000	0.004		0.000	0.005
R^2	**STD for y**	1.000	0.015		1.000	0.012		1.000	0.017
F	**df**	40051	12		71618	12		29023	12

Std A to Std G represent different concentrations, Std A being the highest concentration. LOQ=Limit of Quantification, UCL=Upper calibration limit (for highest three concentrations), b=intercept, m=slope, R^2= The coefficient of determination. F= F statistic, df=degrees of freedom

Table 19. Calibration data for monosaturated carboxylic acids (C_{16}-C_{18})

	Hexadecanoic acid, TMS ester			Heptadecanoic acid, TMS ester			Octadecanoic acid, TMS ester		
	Area / Area IS	Mass [µg/mL]	Area	Area / Area IS	Mass [µg/mL]	Area	Area / Area IS	Mass [µg/mL]	Area
Std G	0.02	0.67	131377	0.01	0.35	47437	0.02	0.68	125855
	0.03	0.67	193385	0.01	0.35	86567	0.03	0.68	191356
Std F	0.03	2.01	184087	0.01	1.04	70749	0.03	2.04	182296
	0.03	2.01	262396	0.02	1.04	124554	0.03	2.04	258547
Std E	0.06	6.02	389597	0.02	3.13	168275	0.06	6.11	396488
	0.06	6.02	500193	0.03	3.13	236957	0.07	6.11	513389
Std D	0.18	18.07	1249512	0.08	9.40	571396	0.19	18.33	1282947
	0.18	18.07	1242063	0.09	9.40	604505	0.18	18.33	1271671
Std C	0.56	54.20	3889509	0.27	28.19	1913284	0.58	54.98	4021803
	0.54	54.20	3678767	0.27	28.19	1798669	0.56	54.98	3825409
Std B	1.59	162.61	10226543	0.82	84.57	5278031	1.65	164.93	10594998
	1.56	162.61	12072363	0.83	84.57	6437502	1.63	164.93	12659284
Std A	4.33	487.84	29502467	2.60	253.72	17691171	4.69	494.79	31964912
	4.23	487.84	31941129	2.55	253.72	19252934	4.55	494.79	34404008
LOQ	**UCL**	0.04	4.28		0.03	2.57		0.05	4.62
m	**b**	0.010	0.012		0.010	-0.0005		0.009	0.0302
STD for m	**STD for b**	0.000	0.005		0.000	0.002		0.000	0.015
R^2	**STD for y**	1.000	0.013		1.000	0.006		0.999	0.046
F	**df**	22186	10		28343	10		15987	12

Std A to Std G represent different concentrations, Std A being the highest concentration. LOQ=Limit of Quantification, UCL=Upper calibration limit (for highest three concentrations), b=intercept, m=slope, R^2= The coefficient of determination. F= F statistic, df=degrees of freedom

Table 20. Calibration data for monosaturated carboxylic acids (C_{19}-C_{21})

	Nonadecanoic acid, TMS ester			Eicosanoic Acid, TMS ester			Heneicosanoic acid, TMS ester		
	Area / Area IS	Mass [µg/mL]	Area	Area / Area IS	Mass [µg/mL]	Area	Area / Area IS	Mass [µg/mL]	Area
Std G	0.003	0.23	17428	0.002	0.22	11685	0.001	0.19	8823
	0.006	0.23	40357	0.005	0.22	34561	0.004	0.19	26760
Std F	0.004	0.69	26708	0.003	0.66	18273	0.002	0.58	12120
	0.007	0.69	52682	0.007	0.66	52773	0.005	0.58	34426
Std E	0.009	2.08	64044	0.006	1.97	43719	0.005	1.75	30933
	0.013	2.08	100393	0.012	1.97	91118	0.008	1.75	66021
Std D	0.035	6.23	239987	0.027	5.92	184747	0.020	5.25	137303
	0.038	6.23	267889	0.034	5.92	237067	0.024	5.25	170134
Std C	0.124	18.70	862326	0.102	17.76	712444	0.078	15.76	542181
	0.125	18.70	851128	0.104	17.76	707076	0.083	15.76	559781
Std B	0.391	56.11	2513721	0.339	53.28	2175019	0.276	47.27	1772480
	0.403	56.11	3121088	0.357	53.28	2765063	0.290	47.27	2250636
Std A	1.371	168.33	9343196	1.233	159.85	8403627	1.116	141.82	7602316
	1.331	168.33	10054769	1.244	159.85	9395577	1.035	141.82	7822887
LOQ	**UCL**	0.02	1.35		0.03	1.24		0.02	1.08
m	**b**	0.007	-0.0027		0.007	-0.0038		0.005	-0.0009
STD for m	**STD for b**	0.000	0.002		0.000	0.003		0.000	0.001
R^2	**STD for y**	0.999	0.005		0.997	0.007		0.991	0.003
F	**df**	9144	10		3429	10		897	8

Std A to Std G represent different concentrations, Std A being the highest concentration. LOQ=Limit of Quantification, UCL=Upper calibration limit (for highest three concentrations), b=intercept, m=slope, R^2= The coefficient of determination. F= F statistic, df=degrees of freedom

Table 21. Calibration data for monosaturated carboxylic acids (C_{22}-C_{24})

	Behenic acid, TMS ester			Tricosanoic acid, TMS ester			Tetracosanoic acid, TMS ester		
	Area / Area IS	Mass [µg/mL]	Area	Area / Area IS	Mass [µg/mL]	Area	Area / Area IS	Mass [µg/mL]	Area
Std G	0.001	0.22	6617	0	0.12	0	0.002	0.20	16186
	0.003	0.22	24527	0	0.12	0	0.002	0.20	16530
Std F	0.001	0.65	9481	0.0003	0.36	1877	0.003	0.61	22888
	0.004	0.65	29566	0.0016	0.36	11918	0.003	0.61	22216
Std E	0.004	1.94	25491	0.0030	1.09	20609	0.006	1.82	41387
	0.008	1.94	60590	0.0027	1.09	20792	0.006	1.82	45255
Std D	0.017	5.82	116191	0.0094	3.26	63833	0.018	5.47	124819
	0.023	5.82	162378	0.0091	3.26	63569	0.018	5.47	125687
Std C	0.073	17.47	508887	0.0367	9.78	255670	0.053	16.42	369452
	0.080	17.47	540783	0.0377	9.78	255980	0.054	16.42	363935
Std B	0.263	52.40	1691846	0.1367	29.34	878099	0.256	49.26	1646562
	0.288	52.40	2235077	0.1171	29.34	908048	0.206	49.26	1599467
Std A	1.040	157.19	7083454	0.4847	88.02	3302630	0.869	147.79	5922518
	1.035	157.19	7822130	0.4376	88.02	3305927	0.788	147.79	5950826
LOQ	**UCL**	0.02	1.04		0.00	0.46		0.00	0.83
m	**b**	0.005	-0.0054		0.004	-0.0025		0.003	0.0010
STD for m	**STD for b**	0.000	0.003		0.000	0.002		0.000	0.000
R^2	**STD for y**	0.993	0.009		0.990	0.005		0.999	0.001
F	**df**	1443	10		1017	10		9836	8

Std A to Std G represent different concentrations, Std A being the highest concentration. LOQ=Limit of Quantification, UCL=Upper calibration limit (for highest three concentrations), b=intercept, m=slope, R^2= The coefficient of determination. F= F statistic, df=degrees of freedom

Table 22. Calibration data for unsaturated carboxylic acids (C_8 and C_{18})

	2-Octenoic acid, TMS ester			Oleic acid. TMS ester		
	Area / Area IS	Mass [µg/mL]	Area	Area / Area IS	Mass [µg/mL]	Area
Std G	0.007	0.17	49098	0.004	0.52	28587
	0.008	0.17	62006	0.008	0.52	58873
Std F	0.011	0.52	72014	0.006	1.56	43852
	0.012	0.52	88677	0.011	1.56	82675
Std E	0.022	1.56	148196	0.015	4.68	100391
	0.022	1.56	174139	0.020	4.68	154390
Std D	0.065	4.68	436660	0.055	14.03	375168
	0.061	4.68	427455	0.058	14.03	405360
Std C	0.185	14.05	1289837	0.183	42.08	1276874
	0.177	14.05	1199327	0.185	42.08	1253775
Std B	0.516	42.16	3315487	0.569	126.24	3655519
	0.514	42.16	3988314	0.577	126.24	4475417
Std A	1.558	126.48	10616693	1.795	378.71	12232785
	1.531	126.48	11569865	1.764	378.71	13327855
LOQ	**UCL**	0.01	1.54		0.03	1.78
m	**b**	0.012	0.0054		0.005	-0.0062
STD for m	**STD for b**	0.000	0.002		0.000	0.003
R^2	**STD for y**	1.000	0.006		1.000	0.011
F	**df**	96082	12		42047	12

Std A to Std G represent different concentrations, Std A being the highest concentration. LOQ=Limit of Quantification, UCL=Upper calibration limit (for highest three concentrations), b=intercept, m=slope, R^2= The coefficient of determination. F= F statistic, df=degrees of freedom

Table 23. Calibration data for dicarboxylic acids (C_8 and C_{10})

		Suberic acid, TMS eter			Sebacic acid, TMS ester	
	Area / Area IS	Mass [µg/mL]	Area	Area / Area IS	Mass [µg/mL]	Area
Std G	0.001	0.19	17276	0.003	0.44	88443
	0.001	0.19	17476	0.004	0.44	108443
Std F	0.001	0.56	25242	0.006	1.31	151206
	0.001	0.56	27242	0.006	1.31	171206
Std E	0.002	1.69	49979	0.011	3.94	305028
	0.002	1.69	51979	0.011	3.94	325028
Std D	0.005	5.06	124732	0.034	11.82	870278
	0.005	5.06	144732	0.032	11.82	890278
Std C	0.014	15.19	358934	0.096	35.47	2454803
	0.014	15.19	378934	0.096	35.47	2654803
Std B	0.039	45.56	1002238	0.333	106.41	8618348
	0.043	45.56	1202238	0.316	106.41	8818348
Std A	0.171	136.68	4103284	1.146	319.22	27464864
	0.166	136.68	4303284	1.135	319.22	29464864
LOQ	**UCL**	0.00	0.17		0.00	1.14
m	**b**	0.001	0.0004		0.003	-0.0015
STD for m	**STD for b**	0.000	0.000		0.000	0.002
r2	**STD for y**	0.996	0.001		0.997	0.007
F	**df**	2502	10		3529	10

Std A to Std G represent different concentrations, Std A being the highest concentration. LOQ=Limit of Quantification, UCL=Upper calibration limit (for highest three concentrations), b=intercept, m=slope, r^2= The coefficient of determination. F= F statistic, df=degrees of freedom

Table 24. Calibration data for ketones (C_{11} and C_{17})

	2-Undecanone			9-Heptadecanone		
	Area / Area IS	Mass [µg/mL]	Area	Area / Area IS	Mass [µg/mL]	Area
Std G	0.004	0.21	25168	0.0001	0.22	780
	0.005	0.21	34132	0.0003	0.22	2196
Std F	0.006	0.63	42340	0.0003	0.66	1925
	0.007	0.63	53578	0.0005	0.66	4102
Std E	0.014	1.89	94667	0.001	1.97	5321
	0.014	1.89	110662	0.001	1.97	8077
Std D	0.042	5.66	282161	0.003	5.92	19536
	0.041	5.66	285381	0.003	5.92	20238
Std C	0.119	16.99	828526	0.010	17.76	66287
	0.119	16.99	806720	0.010	17.76	65083
Std B	0.327	50.96	2097531	0.031	53.28	197013
	0.331	50.96	2565796	0.030	53.28	229926
Std A	0.936	152.89	6376977	0.105	159.84	717226
	0.956	152.89	7218787	0.100	159.84	752342
LOQ	**UCL**	0.00	0.95		0.00	0.10
m	**b**	0.006	0.0041		0.001	-0.0002
STD for m	**STD for b**	0.000	0.001		0.000	0.000
r2	**STD for y**	0.999	0.003		0.999	0.000
F	**df**	14870	10		10880	10

Std A to Std G represent different concentrations, Std A being the highest concentration. LOQ=Limit of Quantification, UCL=Upper calibration limit (for highest three concentrations), b=intercept, m=slope, r^2= The coefficient of determination. F= F statistic, df=degrees of freedom

Table 25. Calibration data for ketones (C_{19} and C_{21})

	10-Nonadecanone			11-Heneicosanone		
	Area / Area IS	Mass [µg/mL]	Area	Area / Area IS	Mass [µg/mL]	Area
Std G	0.002	0.22	11226	0.0001	0.05	726
	0.003	0.22	23553	0.0004	0.05	2931
Std F	0.003	0.65	17626	0.0003	0.14	2166
	0.005	0.65	37239	0.0008	0.14	5830
Std E	0.006	1.95	38096	0.001	0.42	6155
	0.008	1.95	59820	0.001	0.42	9657
Std D	0.022	5.85	147553	0.004	1.25	23878
	0.025	5.85	172600	0.004	1.25	25246
Std C	0.071	17.56	496051	0.014	3.75	94302
	0.070	17.56	475661	0.013	3.75	88514
Std B	0.216	52.67	1385522	0.043	11.25	277966
	0.216	52.67	1677055	0.046	11.25	356679
Std A	0.679	158.00	4626305	0.159	33.74	1082928
	0.675	158.00	5098850	0.153	33.74	1158963
LOQ	**UCL**	0.01	0.68		0.00	0.16
m	**b**	0.004	-0.0020		0.004	-0.0006
STD for m	**STD for b**	0.000	0.001		0.000	0.000
r2	**STD for y**	1.000	0.004		0.997	0.001
F	**df**	44574	12		3209	10

Std A to Std G represent different concentrations, Std A being the highest concentration. LOQ=Limit of Quantification, UCL=Upper calibration limit (for highest three concentrations), b=intercept, m=slope, r^2= The coefficient of determination. F= F statistic, df=degrees of freedom

APPENDIX D

Calibration Plots for the Standards Used

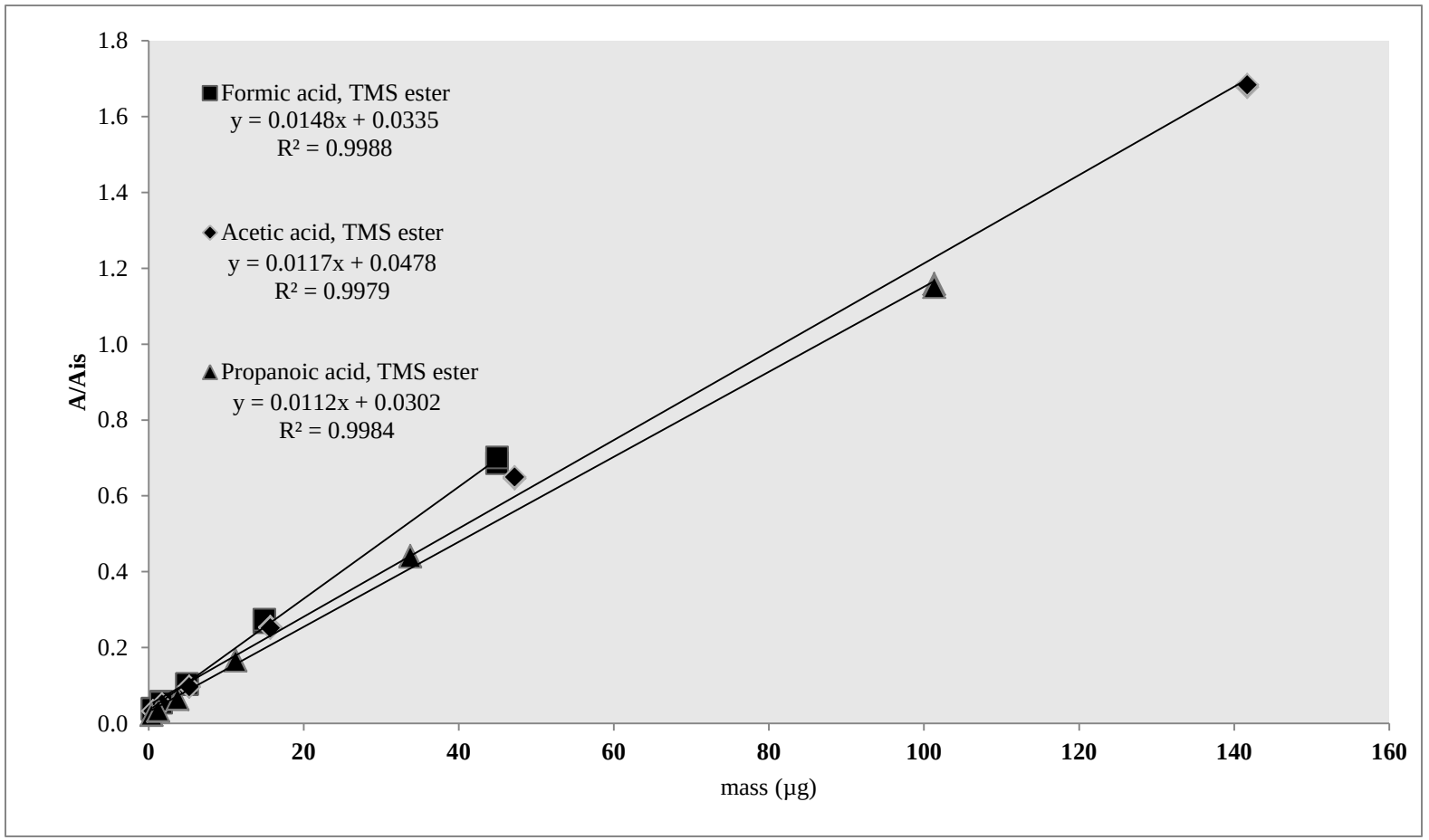

Figure 30. Calibration plots for saturated monocarboxylic acids (C_1-C_3).

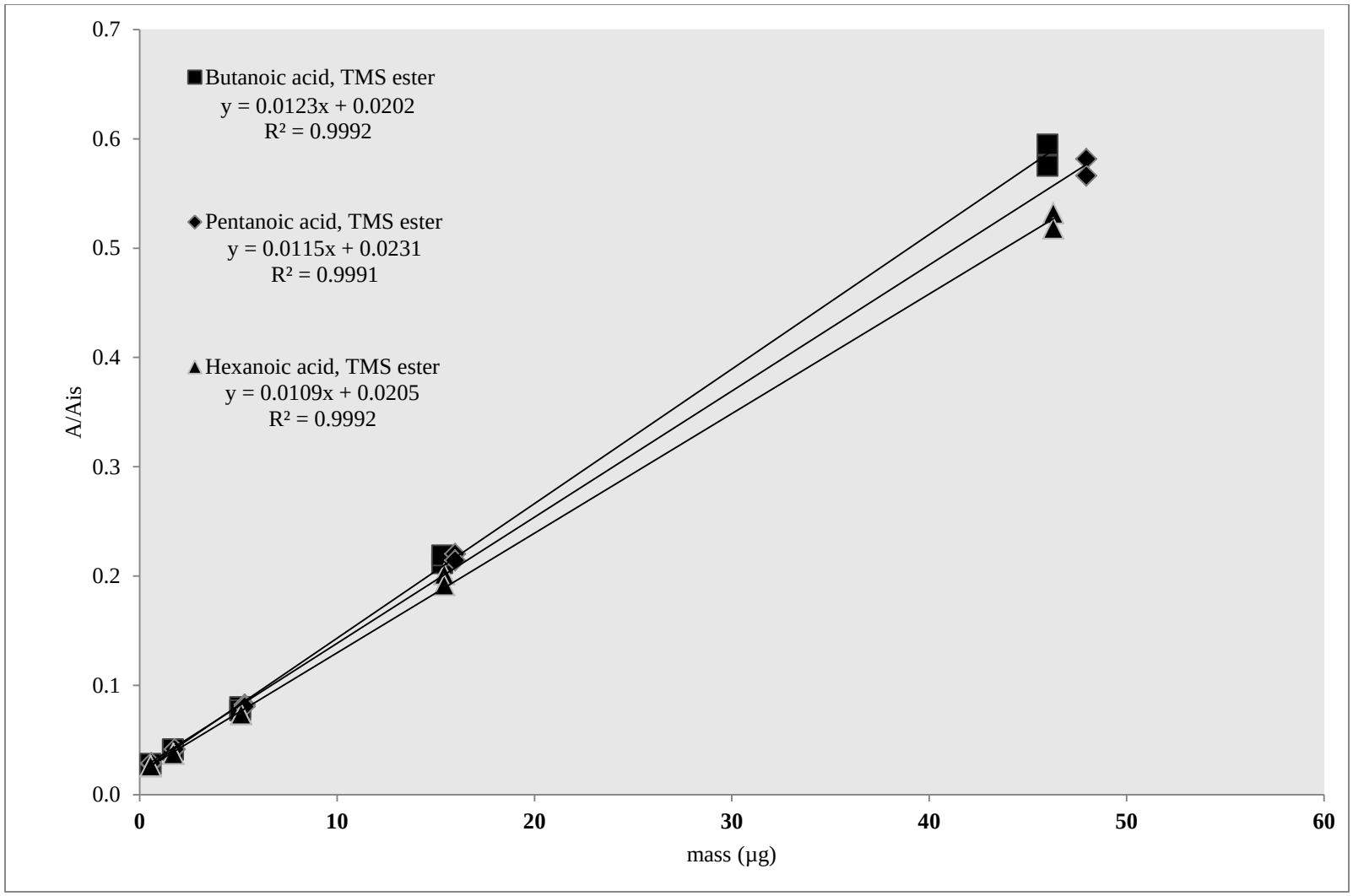

Figure 31. Calibration plots for saturated monocarboxylic acids (C_4-C_6).

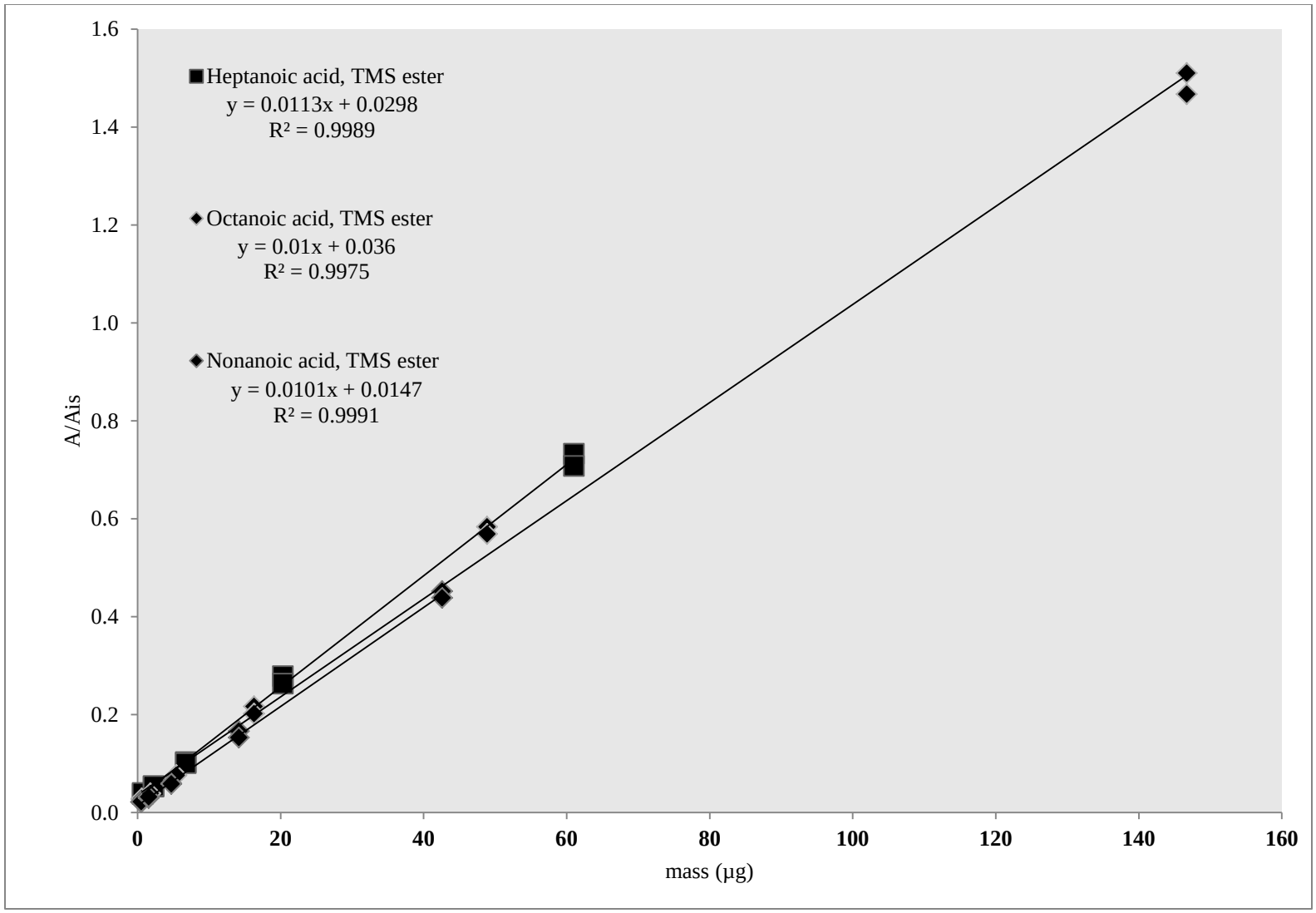

Figure 32. Calibration plots for saturated monocarboxylic acids (C_7-C_9).

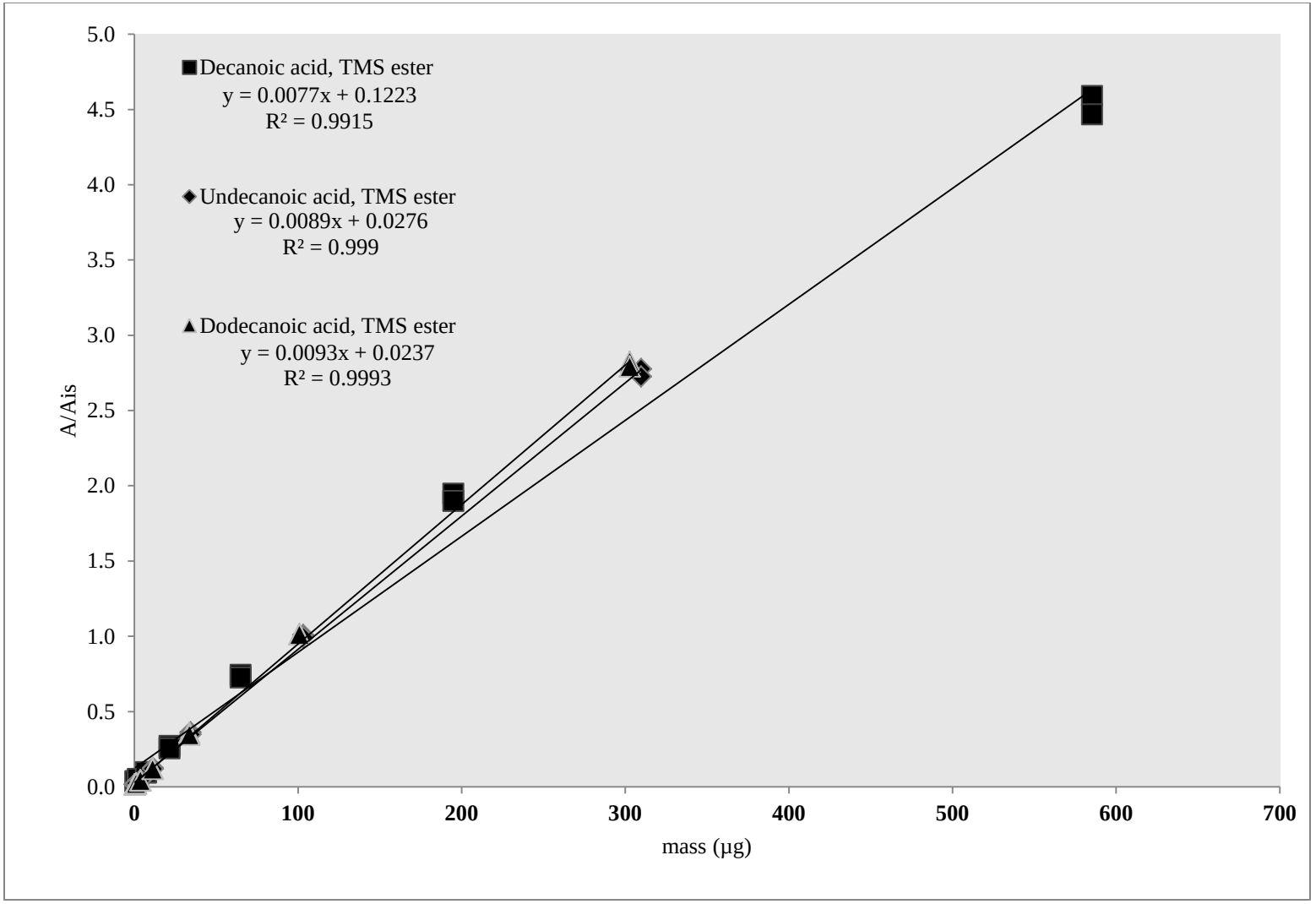

Figure 33. Calibration plots for saturated monocarboxylic acids (C_{10}-C_{12}).

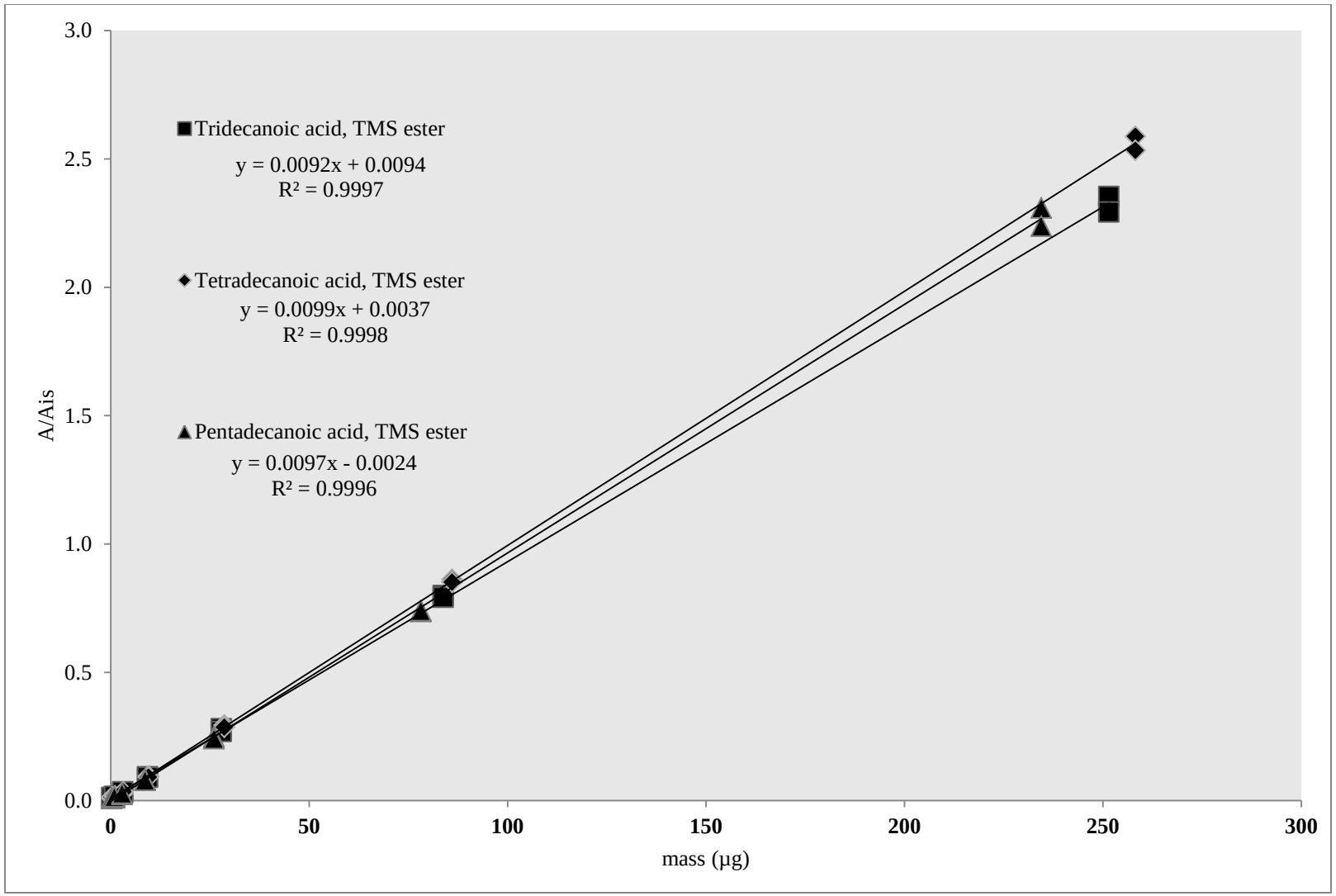

Figure 34. Calibration plots for saturated monocarboxylic acids (C_{13}-C_{15}).

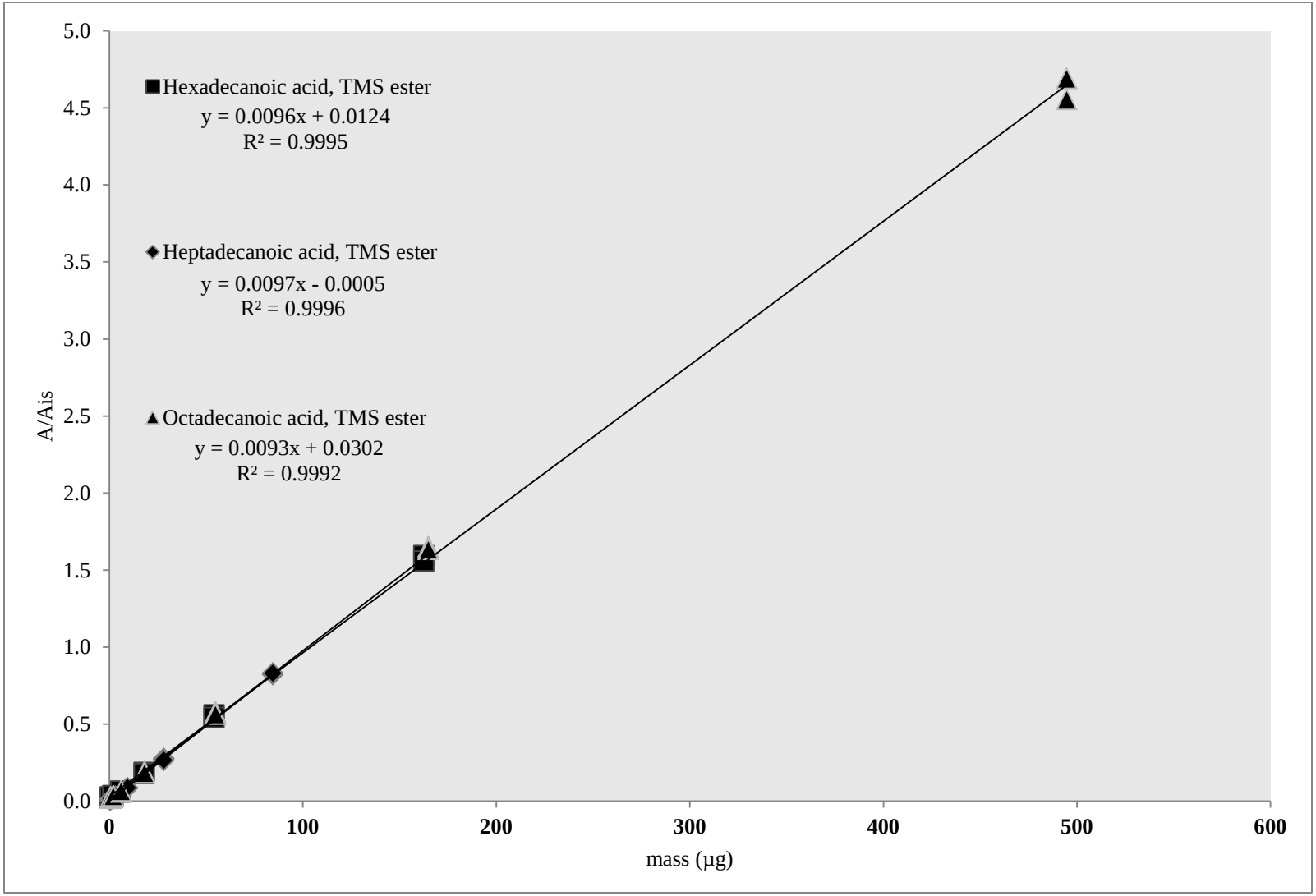

Figure 35. Calibration plots for saturated monocarboxylic acids (C_{16}-C_{18}).

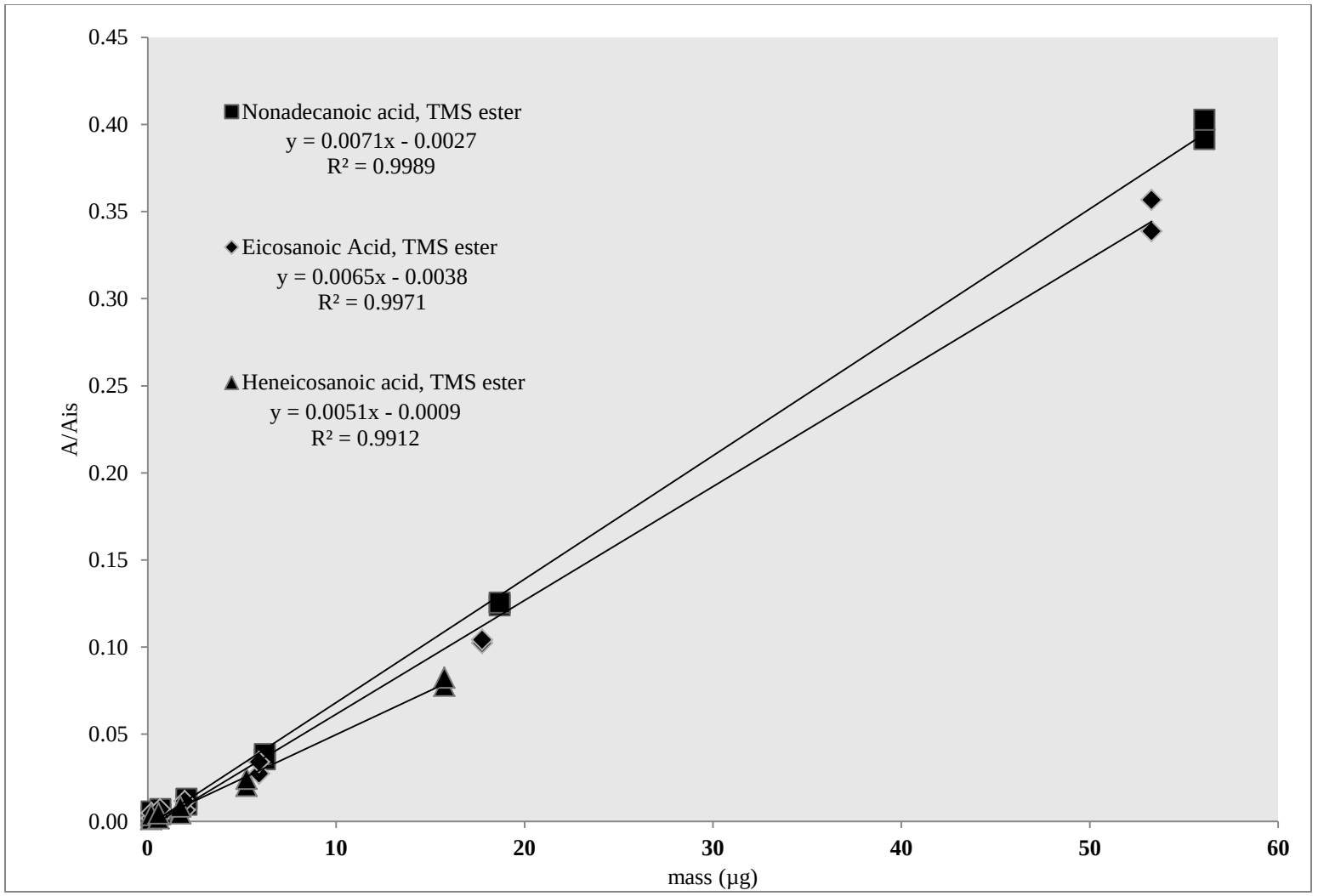

Figure 36. Calibration plots for saturated monocarboxylic acids (C_{19}-C_{21}).

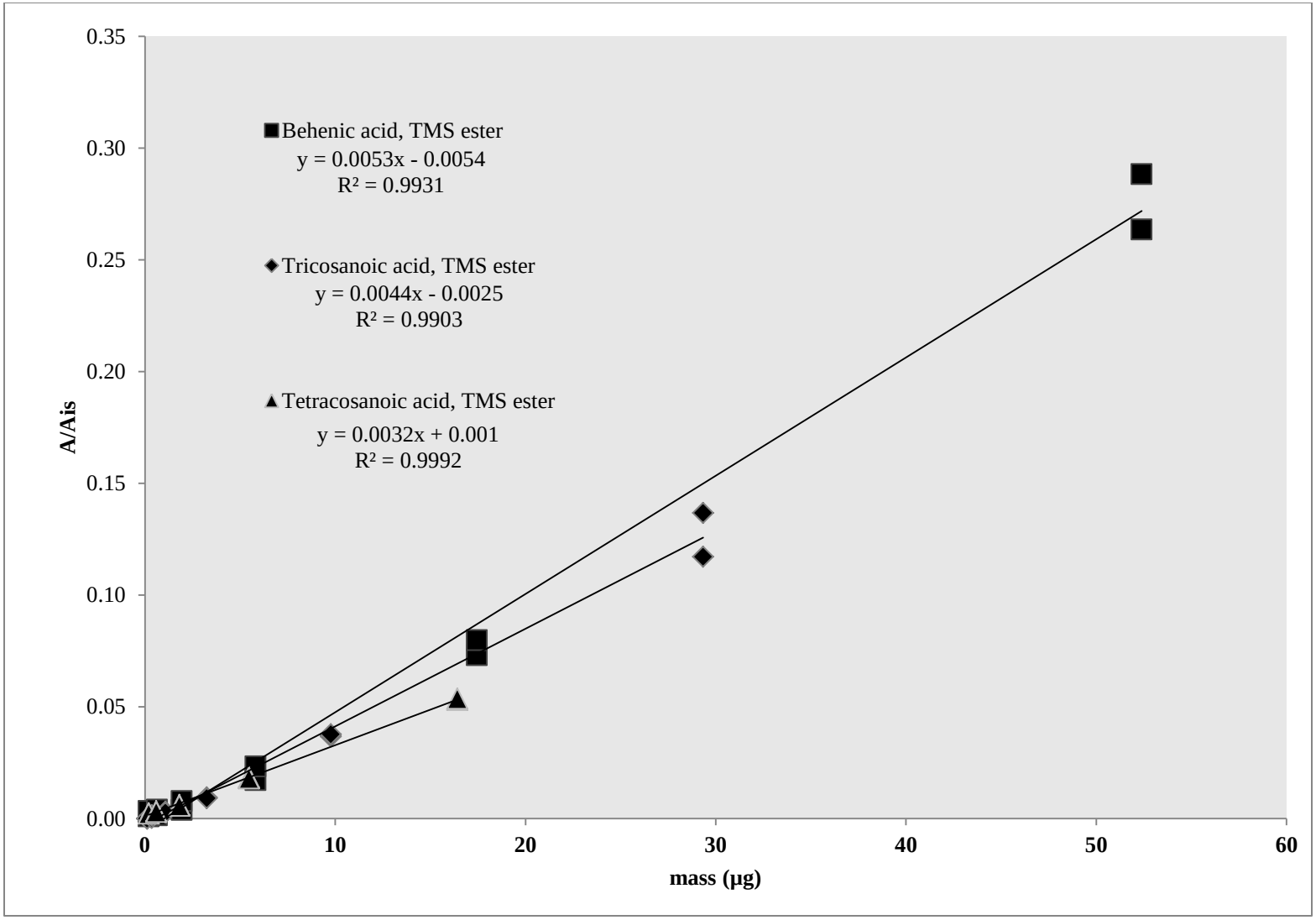

Figure 37. Calibration plots for saturated monocarboxylic acids (C_{22}-C_{24}).

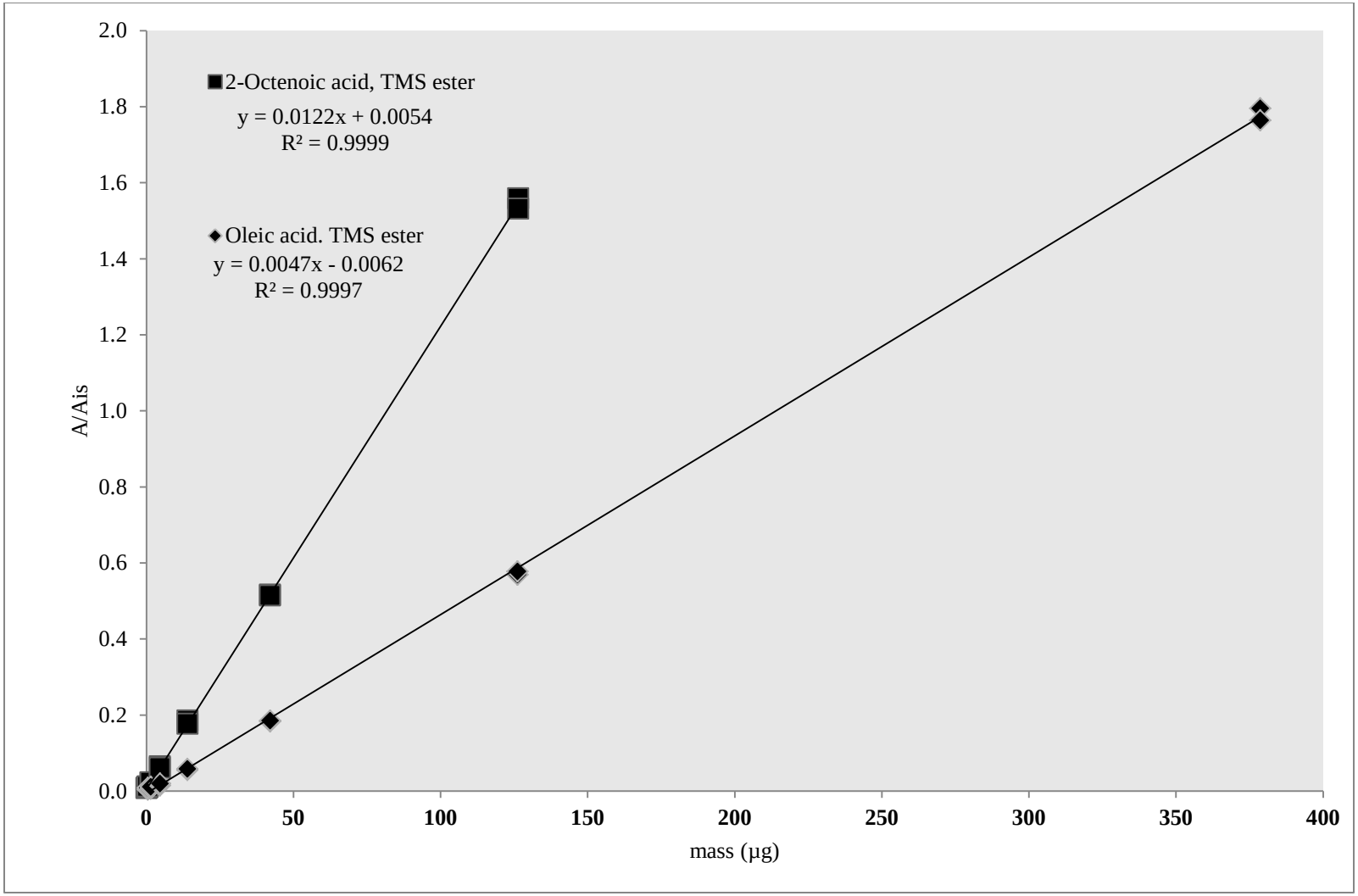

Figure 38. Calibration plots for unsaturated monocarboxylic acids (C_8 and C_{10}).

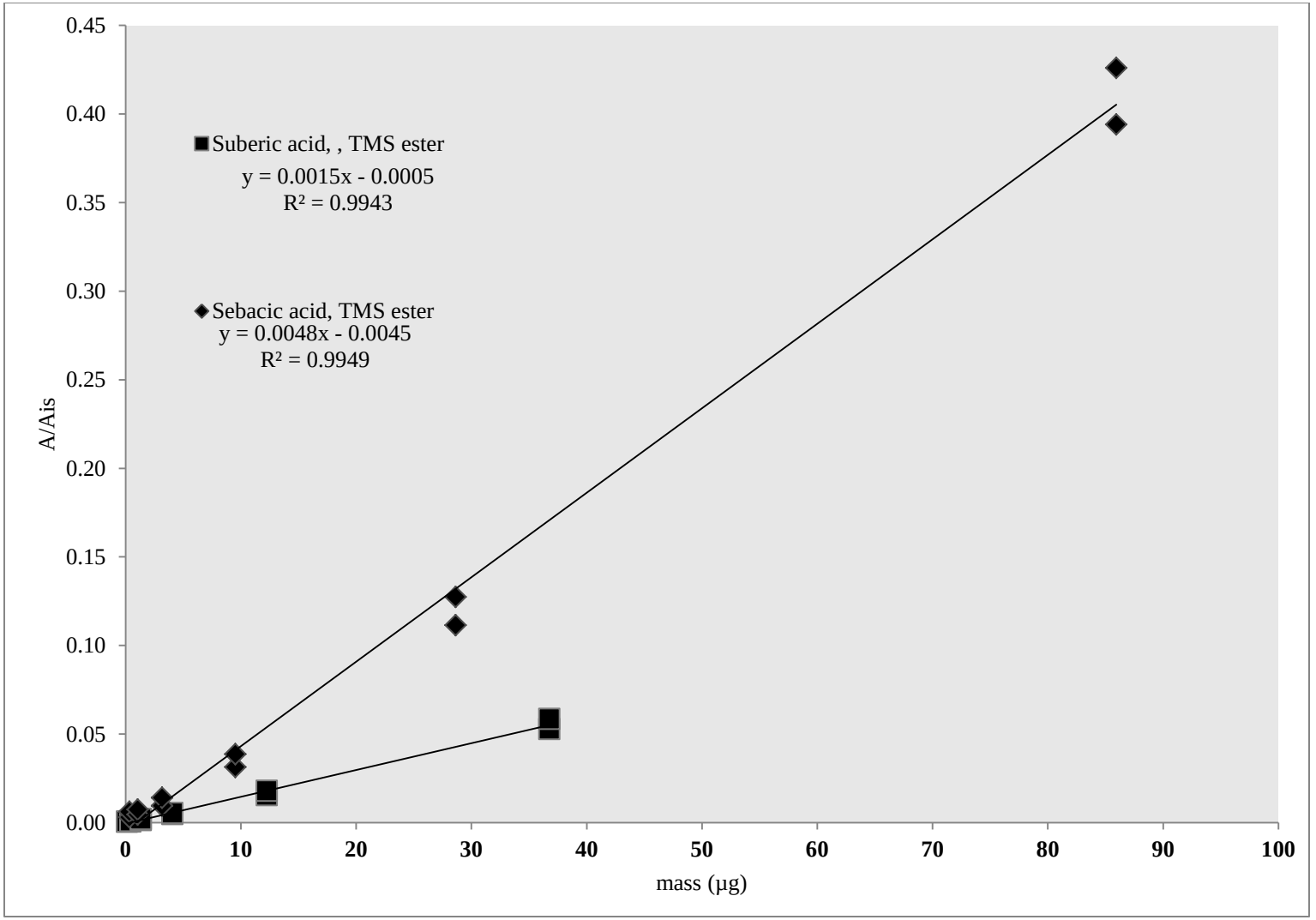

Figure 39. Calibration plots for dicarboxylic acids (C_8 and C_{10}).

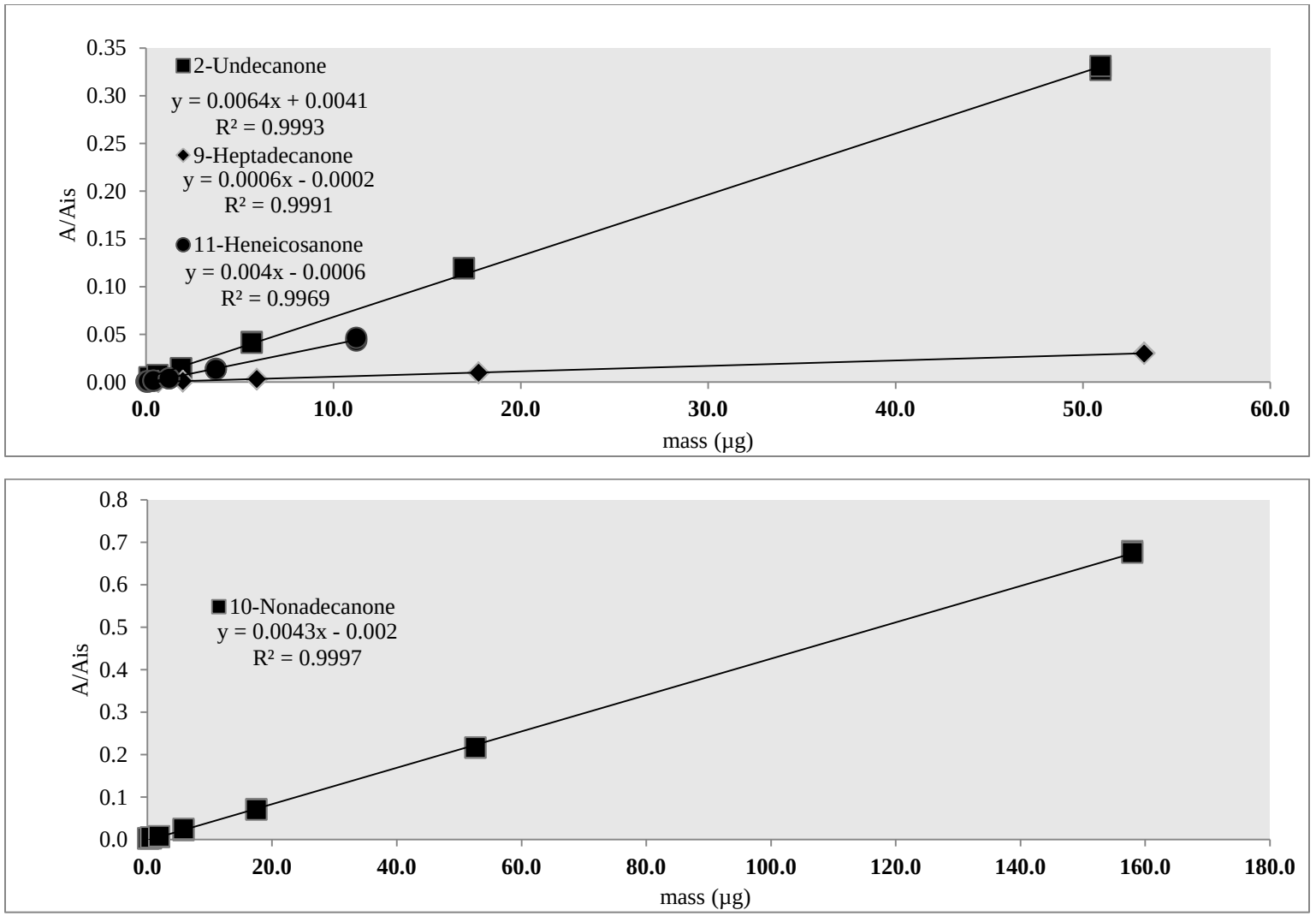

Figure 40. Calibration plots for ketones (C_{11}, C_{17}, C_{19} and C_{21}).

7. REFERENCES

(1) Cadenas, A.; Cabezudo, S. *Technol. Forecast. Soc. Change* **1998**, *58*, 83–103.

(2) Demirbas, A. *Prog. Energy Combust. Sci.* **2007**, *33*, 1–18.

(3) Jefferson, M. *Renew. Energy* **2006**, *31*, 571–582.

(4) Özçimen, D.; Karaosmanoğlu, F. *Renew. Energy* **2004**, *29*, 779–787.

(5) Prasad, S.; Singh, A.; Jain, N.; Joshi, H. C. *Energ. fuel* **2007**, 2415–2420.

(6) Reijnders, L. *Energy Policy* **2006**, *34*, 863–876.

(7) Tore, S.; Uzun, D.; Tore, I. E. *Energy* **1997**, *22*, 17–19.

(8) Buchgraber, M.; Ulberth, F.; Emons, H.; Anklam, E. *Eur. J. Lipid Sci. Technol.* **2004**, *106*, 621–648.

(9) Lestari, S.; Mäki-Arvela, P.; Beltramini, J.; Lu, G. Q. M.; Murzin, D. Y. *ChemSusChem.* **2009**, *2*, 1109–1119.

(10) Srivastava, A.; Prasad, R. *Renew. Sustain. Energy Rev.* **2000**, *4*, 111–133.

(11) Doll, K. M.; Sharma. B. K,; Suarez. A. Z.; Erhan. S. H. *Energ. fuel* **2008**, *257*, 2061–2066.

(12) Yu, W.-L.; Ansari, W.; Schoepp, N. G.; Hannon, M. J.; Mayfield, S. P.; Burkart, M. D. *Microb. Cell Fact.* **2011**, *10*, 91.

(13) Agarwal, A. K. *Prog. Energy Combust. Sci.* **2007**, *33*, 233–271.

(14) Demirbas, A. *Energy Convers. Manag.* **2008**, *49*, 2106–2116.

(15) White, J. E.; Catallo, W. J.; Legendre, B. L. *J. Anal. Appl. Pyrolysis* **2011**, *91*, 1–33.

(16) Canakci, M.; Sanli, H. *J. Ind. Microbiol. Biotechnol.* **2008**, *35*, 431–441.

(17) Demirbas, A. *J. Anal. Appl. Pyrolysis* **2004**, *71*, 803–815.

(18) Bridgwater, A . *Chem. Eng. J.* **2003**, *91*, 87–102.

(19) http://www.chamco.net/Gasification.htm. Accessed on 02/12/2014.

(20) Bridgwater, A. V. *J. Anal. Appl. Pyrolysis* **1999**, *51*, 3–22.

(21) Onay, O.; Kockar, O. M. *Renew. Energy* **2003**, *28*, 2417–2433.

(22) Chang. C. C.; Wan. S.W. *Ind. Eng. Chem* **1947**, *39*, 1543–1548.

(23) Alencar. J. W.; Alves. P. B.; Craveiro. A. A. *J. Agr. Food Chem.* **1983**, *31*, 1268–1270.

(24) Idem, R. O.; Katikaneni, S. P. R.; Bakhshi, *Energ. fuel*. **1996**, *10*, 1150–1162.

(25) http://www.canolainfo.org/quadrant/media/downloads/pdfs /classicandhighole iccanolaoils.pdf. Accessed on 02/12/2014.

(26) Dupain, X.; Costa, D. J.; Schaverien, C. J.; Makkee, M.; Moulijn, J. A. *Appl. Catal. B Environ.* **2007**, *72*, 44–61.

(27) Maher, K. D.; Bressler, D. C. *Bioresour. Technol.* **2007**, *98*, 2351–2368.

(28) http://www.mhhe.com/physsci/chemistry/carey/student/olc/ ch19reaction carboxylicacids.html. Accessed on 02/12/2014.

(29) Kubičková, I.; Snåre, M.; Eränen, K.; Mäki-Arvela, P.; Murzin, D. Y. *Catal. Today* **2005**, *106*, 197–200.

(30) Kubickova, I.; Snåre, M.; Era, K.; Murzin, D. Y.; Uni, V.; Turku, F.; September, R. V; Re, V.; Recei, M.; October, V. *Energ. Fuels* **2007**, *21*, 30–41.

(31) Kubátová, A.; Luo, Y.; Šťávová, J.; Sadrameli, S. M.; Aulich, T.; Kozliak, E.; Seames, W. *Fuel* **2011**, *90*, 2598–2608.

(32) Kubátová, A.; Sťávová, J.; Seames, W. S.; Luo, Y.; Sadrameli, S. M.; Linnen, M. J.; Baglayeva, G. V.; Smoliakova, I. P.; Kozliak, E. I. *Energ. Fuels* **2012**, *26*, 672–685.

(33) Šťávová, J.; Beránek, J.; Nelson, E. P.; Diep, B. A; Kubátová, A. *J. Chromatogr. B* **2011**, *879*, 1429–1438.

(34) Sťávová, J.; Stahl, D. C.; Seames, W. S.; Kubátová, A. *J. Chromatogr. A* **2012**, *1224*, 79–88.

(35) Boateng, A. A.; Anderson, W. F.; Phillips, J. G. *Energ. Fuels* **2007**, *47*, 1183–1187.

(36) Luo, Y.; Ahmed, I.; Kubátová, A.; Šťávová, J.; Aulich, T.; Sadrameli, S. M.; Seames, W. S. *Fuel Process. Technol.* **2010**, *91*, 613–617.

(37) Kozliak, E.; Mota, R.; Rodriguez, D.; Overby, P.; Kubátová, A.; Stahl, D.; Niri, V.; Ogden, G.; Seames, W. *Ind. Crops Prod.* **2013**, *43*, 386–392.

(38) http://www.hort.purdue.edu/newcrop/ncnu02/v5-055.html. Accessed on 02/12/2014.

(39) Moser, B. R. *Lipid Technol.* **2010**, *22*, 270–273.

(40) http://www.hort.purdue.edu/newcrop/proceedings1993../V2-314.html Accessed on 02/12/2014.

(41) Haas, M. J. *Fuel Process. Technol.* **2005**, *86*, 1087–1096.

(42) Schwab, A. W.; Dykstra, G. J.; Selke, S. C. *J. Am. Oil Chem. Soc.* **2014**, 1–8.

(43) http://www.cottonseed.com/publications/csobro.asp Accessed on 02/12/2014.

(44) Cermak, S. C.; John, A. L.; Evangelista, R. L. *Ind. Crops Prod.* **2007**, *26*, 93–99.

(45) http://www.canolainfo.org/quadrant/media/downloads/pdfs /classicandhighole iccanolaoils.pdf. Accessed on 02/12/2014.

(46) http://www.brenntagspecialties.com/en/downloads/Products/Personal_care/ Textron/PDS_JOJOBA_OIL_CLEAR_TX008192.pdf. Accessed on 02/12/2014.